HEAT TRANSFER IN ANNULAR PASSAG

TURBULENT FORCED CONVECTION HEAT TRANSFER

IN

ANNULAR PASSAGES

By

ROSS LEONARD JUDD, B.E.Sc.

A Thesis

Submitted to the Faculty of Graduate Studies

in Partial Fulfilment of the Requirements

for the Degree

Master of Engineering

McMaster University

May 1963

MASTER OF ENGINEERING (1963)
(Mechanical Engineering)

McMASTER UNIVERSITY
Hamilton, Ontario.

TITLE: Turbulent Forced Convection Heat Transfer in Annular Passages

AUTHOR: Ross Leonard Judd, B.E.Sc. (University of Western Ontario)

SUPERVISOR: Doctor J. H. T. Wade

NUMBER OF PAGES: vi, 61.

SCOPE AND CONTENTS:

An experimental study of turbulent forced convection heat transfer to water flowing in a vertical annular passage is reported in this paper. The study investigates the influence of eccentricity (ranging from 0% to 80%) and diameter ratio (ranging from 1.5 to 4.0) upon the heat transfer phenomena occurring at the inner boundary of the annular passage.

Dimensionless heat transfer parameters calculated from measurements made at the two locations corresponding to the maximum and minimum separation of the inner and outer boundaries of the annular passage are correlated in terms of the Reynolds number, the eccentricity and the diameter ratio. Analysis of the correlations indicates that eccentricity affects the heat transfer phenomena occurring at the two locations on the inner boundary of the annular passage in different fashions; increasing eccentricity causes the heat transfer to increase at the location corresponding to the maximum separation of the boundaries and causes the heat transfer

to decrease at the location corresponding to the minimum separation of the boundaries. The magnitude of the increase or decrease in heat transfer is dependent upon the diameter ratio; at a particular level of eccentricity, the greater variations in heat transfer occur at the smaller diameter ratios. Ranges in which eccentricity does not influence heat transfer are found in connection with the larger diameter ratios.

Moody friction factors calculated from measurements made with concentric annular passages are correlated as a function of Reynolds number.

ACKNOWLEDGEMENTS

The author gratefully acknowledges the assistance and support of Doctor J. H. T. Wade who provided guidance and advice in planning and performing the experimental study.

The experimental study reported in this paper was partially financed by National Research Council Grant A-1585.

TABLE OF CONTENTS

LIST OF FIGURES

TEXT

1. INTRODUCTION

Although convective heat transfer in annular passages has many applications in the design of industrial heat transfer equipment, the information available in the literature concerning heat transfer in such systems is relatively incomplete. There is little available information concerning the effect of eccentricity upon forced convection heat transfer; and the information which is available is not adequate to quantitatively assess the influence of diameter ratio upon forced convection heat transfer in annular passages. Those investigators who have studied forced convection heat transfer in eccentric annular passages have generally covered the complete range of eccentricities but have not explored the range of diameter ratios in sufficient detail.

The present paper describes an experimental study investigating the influence of eccentricity (ranging from 0% to 80%) and diameter ratio (ranging from 1.5 to 4.0) upon forced convection heat transfer to water at the inner boundary of a vertical annular passage. The experimental study was comprised of tests upon nineteen annular test configurations involving various combinations of five levels of eccentricity and six levels of diameter ratio. Heat transfer results were evaluated at the two locations corresponding to the maximum and minimum separation of the inner and outer boundaries of the annular passage.

Correlations are presented enabling the local heat transfer coefficients existing at the two locations on the inner boundary of the annular passage to be evaluated numerically. The results of other investigations have shown that average heat transfer coefficients in eccentric annular passages do not vary appreciably from average heat transfer coefficients in concentric annular passages and for this reason, average heat transfer coefficients are not presented. The singular function of the information presented is the prediction of local heat transfer coefficients on the inner boundary of annular passages. Heat transfer at the location corresponding to the minimum separation of the boundaries is of particular interest because this is the location where excessively high surface temperatures are liable to occur.

In addition, the present paper describes an experimental study investigating the influence of eccentricity (ranging from 0% to 80%) and diameter ratio (ranging from 1.5 to 2.5) upon pressure drop for turbulent flow in a vertical annular passage. A correlation is presented enabling the pressure drop in concentric annular passages to be evaluated numerically for the particular value of relative roughness involved.

2. LITERATURE SURVEY

The influence of diameter ratio upon the transfer of heat from the inner boundary of a concentric annular passage was first investigated by Foust and Christian (1). From the results of their experiments involving the transfer of heat to water flowing in ten different annular passages with diameter ratios varying from 1.20 to 2.36, Foust and Christian were able to prove the dependence of the heat transfer process upon diameter ratio. Subsequently, Monrad and Pelton (2) investigated the transfer of heat to water flowing in three annular passages with diameter ratios 1.65, 2.45 and 17 and derived the following correlation

$$Nu_B = 0.020\ (Re_B)^{0.8}\ (Pr_B)^{1/3}\ (D_o/D_i)^{0.53}$$

relating the heat transfer coefficients at the inner boundary of the annular passage to the flow conditions and fluid properties existing in the passage. For water flowing through a vertical annular passage with diameter ratio 1.33, Carpenter, Colburn, Schoenburn and Wurster (3) were able to derive an equivalent correlation involving the viscosity ratio (μ/μ_S). Stein and Begell (4) thoroughly investigated the transfer of heat to water flowing in three annular passages with diameter ratios 1.25, 1.50 and 1.75 and derived the correlation

$$St_F\ (Pr_F)^{2/3}\ (Re_F)^{0.2}\ (D_o/D_i)^{0.5} = 0.0200$$

which is essentially the correlation derived by Monrad and Pelton.

Deissler and Taylor (5) have extended a previous theoretical analysis for turbulent velocity and temperature distributions in tubes to predict turbulent velocity and temperature distributions in an annular passage. Using the theoretical relationship derived, Deissler and Taylor have predicted the average heat transfer coefficient and the circumferential variation of the local heat transfer coefficient for air flowing through an annular passage with diameter ratio 3.5 and various eccentricities within the range 0% to 100%. The theoretical results presented by Deissler and Taylor indicate extreme variations in heat transfer coefficient around the inner boundary of the annular passage which are inconsistent with the variations measured by other investigators.

Heyda (6) has developed an analytical procedure based upon a continuous velocity distribution for turbulent flow near a smooth wall derived by Van Driest to determine the temperature field in an eccentric annular passage. Since Heyda has not applied the analytical procedure to solve a practical example, the validity of the theory is unknown.

Diskind (7) has reported the results of an experimental study performed at Columbia University in which the influence of eccentricity upon turbulent forced convection heat transfer and pressure drop in an annular passage with diameter ratio 1.5 was investigated. Water passed vertically upward through an annular passage in which the relative location of the inner and outer boundaries could be changed. The inner boundary of the annular passage was electrically heated. Heat transfer coefficients and friction factors were calculated from measurements of the resulting temperature and pressure distributions.

Diskind has presented average heat transfer coefficients with sufficient additional information to evaluate the circumferential variation in local heat transfer coefficients.

Fauré (8) has reported the results of a similar study performed in France in which the influence of eccentricity upon turbulent forced convection heat transfer and pressure drop in three annular passages with diameter ratios 2.3, 3.3 and 5.4 was investigated. Air flowing vertically through an annular passage was heated by an electrically heated tube forming the inner boundary of the annular passage. The relative location of the inner and outer boundaries could be changed, enabling the eccentricity of the annular passage to be varied. Heat transfer coefficients and friction factors were calculated from measurements of the resulting temperature and pressure distributions. Fauré has presented average heat transfer coefficients and the circumferential variation in local heat transfer coefficients for surface temperatures ranging from 80°C to 800°C. In support of these heat transfer results, Fauré has presented velocity and temperature profiles measured within the annular passage for both concentric and eccentric arrangements of the boundaries of the annular passage.*

The experimental results presented by Diskind and Fauré are in general agreement; the dependence of heat transfer coefficient upon eccentricity in each case is similar, although a direct comparison cannot be made because of differences in diameter ratios. However,

---

*Reference (9), an English translation of reference (8) can be obtained from the Department of Mechanical Engineering, McMaster University.

the theoretical results presented by Deissler and Taylor are not in agreement with the experimental results presented by either Diskind or Fauré in that the variation in theoretically calculated local heat transfer coefficients is several times greater than the variation in experimentally measured local heat transfer coefficients. The assumptions which Deissler and Taylor have employed in developing their theoretical relationship are therefore suspect.

3. TEST FACILITY

A photograph of the test facility used in performing the experimental study is shown in Figure 1. The components comprising the test facility were arranged to form a closed system, such that the fluid upon which the heat transfer experiments were performed (water) circulated continuously through a pump section, a heater section, a flow meter section, a test section and a cooler section. The arrangement of the various components is shown schematically in Figure 2.

For purposes of description, the test facility may be considered to be comprised of two assemblies, the test rig and the test section. The function of the test rig was to provide the test section with water at a regulated flowrate and temperature; the function of the test section was to establish velocity and temperature distributions in the water for various annular test configurations and to evaluate the corresponding surface heat transfer coefficients.

3.1 Test Rig

A Worthington model 6GAU gear pump operating at 1750 revolutions/minute discharged water at a constant rate of 55 U.S. gallons/minute for any pressure up to 50 pounds/square inch which was the pressure at which the automatic relief valve within the pump opened. The portion of the flowrate in excess of that required for a particular test was recirculated through the pump by means of an external pump bypass, enabling the rate of flow through the system to be controlled by the setting of a manually operated valve. This method of control proved to be quite adequate, as the flowrate responded quickly to changes in valve setting and fluctuations in flowrate were negligible.

Heat was added to the water in the system as it circulated through the heater section. The heat source was a Chromalox model TM612 flanged pipe heater comprised of six calrod elements, each having a rated 2000 watt heat output at 230 volts. The temperature of the water could be regulated by the manually operated heater controls which were so connected that the total heat output could be varied continuously from 0 watts to 12,000 watts. The operation of the heater section was typical of this type of heat transfer equipment in that relatively long periods of time were required to effect a change in temperature after a change in the control setting. However it proved possible to predict system heat requirements for particular test conditions, enabling the heater section to be operated satisfactorily.

The water flowrate was measured in a calibrated flow meter section employing an orifice plate designed in accordance with the British Standard Code for Flow Measurements (B.S. 1042:1943). The flow meter section, comprised of a length of straight pipe upstream of the orifice plate, the orifice plate and a length of straight pipe downstream of the orifice plate was calibrated twice during the experimental study. The range of flowrates which the flow meter section was required to measure induced differential pressures across the orifice plate varying in magnitude by a factor of twenty. The inaccuracies associated with the measurement of the smaller differential pressures reduced the precision with which the smaller flowrates could be measured.

Heat was removed from the water as it circulated through the cooler section. The heat sink was a Heliflow model 9XF-16S heat exchanger in which heat was exchanged with mains water. The temperature of the water could be regulated by controlling the flow of mains water with two valves which were installed in parallel upstream of the cooler section for this purpose; the larger valve provided coarse control and the smaller valve provided fine control. This method of control proved to be quite satisfactory in that the rate of heat exchange could be precisely set and maintained. An orifice plate was installed upstream of the control valves, enabling the mains water flowrate to be measured so that particular test conditions could be re-established.

A 5 U. S. gallon capacity head tank was connected in the system upstream of the pump section to accommodate expansion of the water. The head tank was mounted higher than any other point in the system in order to keep the system flooded during operation and was vented at the top in order to establish atmospheric pressure in the system upstream of the pump section.

3.2 Test Section

The manner in which the components comprising the test section were assembled is illustrated in Figure 3. An annular passage through which the water circulated was formed between the inner tube assembly and the outer tube assembly. The 0.50" O.D. inner tube assembly, which was common to all the configurations investigated formed the inner boundary of the annular passage; one of six outer tube assemblies having diameters ranging from 0.75" I.D. to 2.00" I.D. formed the outer boundary of the annular passage.

Inspection of Figure 3 will reveal that the inner tube assembly was mounted eccentrically in the housings and that the outer tube assembly was mounted eccentrically in the hubs. This offset, which was identical in each case, enabled the eccentricity of the annular passage to be varied. The hubs supporting the outer tube assembly could be rotated with respect to the housings, carrying the axis of the outer tube assembly around the circumference of a circle. As the outer surfaces of the hubs were concentrically mounted with respect to the true axes of the housings, the axis of the inner tube assembly intersected the circle representing the locus of the axis of the outer tube assembly. Consequently, any separation of the axes of the inner tube assembly and outer tube assembly could be achieved simply by rotating the hubs. When the hubs were so aligned that the axis of the outer tube assembly coincided with the axis of the inner tube assembly, concentricity was obtained.

The effective length of the inner tube assembly consisted of a stainless steel tube 0.50" O.D. x 0.010" W.T. x 24" long which was heated by a heavy electric current. Tests performed upon similar pieces of tubing had indicated that the variations in wall thickness and resistivity of the stainless steel tube were small and consequently, the heat generation per unit surface area could be considered uniform.

Copper tubes 0.50" O.D. x 0.375" I.D. were silver brazed to the stainless steel tube in order to extend its length and to create an unheated length in which fully developed turbulent flow could be established. The copper tubes conducted the electric current to and from the effective length. The relative resistivities and cross sections of the tubes were such that heat generation in the copper tubes did not exceed 0.5% of the heat generation in the stainless steel tube.

The outer tube assemblies were fabricated from stock plastic tubes. Six sets of hubs, one for each outer tube assembly were machined from sheet plastic. The outer tube assemblies were mounted in the hubs on rubber "O" rings which enabled the outer tube assemblies to be rotated about their respective axes. Each outer tube assembly was fitted with two sets of diametrically opposed pressure taps which spanned the effective length and three dial indicator mountings located in line with the pressure taps.

In order to maintain the eccentricity uniform over the length of the test section, support legs were mounted on the inner tube assembly upstream and downstream of the effective length. The support legs consisted of lengths of 1/8" diameter plastic rod threaded into specially machined supporting rings which were soft soldered to the inner tube assembly. The plastic legs were machined to length in accordance with the particular outer tube assembly and separation being investigated in order to locate the inner tube assembly precisely with respect to the outer tube assembly*.

*The theory derived for calculating support leg length is presented in Appendix 2.

In order to confirm the eccentricity of a particular configuration, measurements of the actual separation of the boundaries of the annular passage were made. A dial indicator with a 2" travel was mounted in turn in each of the three dial indicator mountings, clamped in place and rotated with the outer tube assembly about its axis. The stem of the dial indicator rode on the inner tube assembly and indicated a deflection equivalent to twice the separation of the axes of the inner tube assembly and outer tube assembly for one complete revolution. These measurements enabled the actual eccentricities to be calculated at three positions in the effective length.

The power supply for the test section was a Miller model SR 1000 B1 direct current welding transformer. The heat generation in the test section could be regulated by the control provided with the machine enabling stepless continuous variation in heat generation from 1 kilowatt to the specified value. The capacity of the welding transformer and the voltage-current characteristics of the stainless steel tube were such that a maximum heat generation of approximately 45 kilowatts (900 amperes at 50 volts) could have been obtained. However, the cables used limited the current, and as a consequence the heat generation in the experimental study did not exceed 14 kilowatts (520 amperes at 28 volts). The use of this welding transformer as a power source proved quite satisfactory in that any specified heat flux could be achieved simply by setting the control on the welding transformer.

3.3 Test Instrumentation

This section discusses at length the various instruments used in measuring the test conditions pertinent to the investigation of turbulent forced convection heat transfer in an annular passage.

The various temperatures in the test section were measured with eighteen thermocouples, three of which were stream thermocouples immersed in the water upstream of the effective length, twelve of which were surface thermocouples spotwelded to the inner surface of the stainless steel tube comprising the effective length and three of which were stream thermocouples immersed in the water downstream of the effective length. The twelve thermocouples spot welded to the inner surface of the stainless steel tube were positioned along the length of the tube in two diametrically opposite groups at four inch intervals spaced alternately. The location of the thermocouples in the test section is shown schematically in Figure 4.

The thermoelectric potentials of these eighteen thermocouples were recorded on a Philips model PR 3210 A/00 twelve point self balancing millivolt recorder. The thermoelectric potentials of the six stream thermocouples were recorded continuously; a switching circuit was arranged enabling the thermoelectric potentials of either group of surface thermocouples to be recorded depending upon the arbitrary setting of a switch. The thermoelectric potentials of all eighteen thermocouples were referenced to ice temperature.

The six stream thermocouples were formed from Thermoelectric "Ceramo" miniature sheathed thermocouple wire with inert oxide insulation. The type "J" iron-constantan pair contained by the sheath was welded together and grounded to the sheath at the hot junction. The twelve surface thermocouples were formed from Thermoelectric "Fibreglass-Fibreglass" thermocouple wire treated with high temperature varnish. The type "J" iron-constantan pair in the thermocouple wire was spotwelded together and then spotwelded in position using a specially developed fixture. The leads from the twelve surface thermocouples and the leads from the three stream thermocouples downstream of the effective length were brought out through the copper tube and terminated in a junction box at the downstream end of the test section; the leads from the three stream thermocouples upstream of the effective length were brought out through the copper tube and terminated in a junction box at the upstream end of the test section. The rated accuracy of the thermocouples used was $\pm$ 3/4% of the temperature measurement, giving a possible 1.5°F error in the difference of the measurements of the surface thermocouples and the stream thermocouples.

The bulk temperature of the water entering and leaving the test section was measured with two precision mercury-in-glass thermometers which could be read to 0.1°F. The thermometers, which were used in determining the rise in bulk temperature of the water circulating through the test section, were installed in thermometer wells located upstream and downstream of the test section. The precision with which the thermometers could be read produced a possible 0.2°F error in the calculation of the bulk temperature rise.

The heat generated in the test section was calculated from measurements of the potential drop over the test section and the current flowing through the test section. A Metra model DLi No. 62262 variable range voltmeter with a rated accuracy of ± 1% of the full scale value measured the potential drop over the test section; a Simpson model 29SC-No. 10028 ammeter-shunt combination with a rated accuracy of ± 1% of the full scale value measured the current flowing through the test section. Using the measurements of these instruments, the maximum possible error in the calculation of the heat generated in the test section was approximately ± 5%.

The differential pressures induced by the flow through the orifice in the flow meter section and by the flow through the orifice in the mains water line were measured with 16" differential mercury manometers. The scales with which the manometers were fitted enabled differential pressures to be measured to ± 0.05 inches of mercury. The maximum possible error in the corresponding flowrate measurement was approximately ± 5%.

The pressure drop over the effective length of the test section was measured with two 36" differential mercury manometers. The differences in mercury columns could be measured to ± 0.05 inches, giving a maximum possible error in the measurement of pressure drop of approximately ± 10%.

The system pressure at the pump discharge was measured with a U. S. Gauge Company bourdon tube pressure gauge which was calibrated with a dead weight tester before being put into service. On the basis of this calibration, the maximum possible error associated with the use of this gauge to measure system pressure was assumed to be ± 10%.

The ambient temperature in the vicinity of the test facility was measured with a precision mercury in glass thermometer.

4. EXPERIMENTAL PROCEDURE

No special attempt was made to maintain the purity of the water circulating in the system. Prior to each test, the system was refilled with water from the mains. During filling, air trapped in the system was bled off at the test section and the heater section where bleed points for this purpose had been provided.

After the system had been filled, the water was circulated and a drain was opened permitting mains water to purge the system. It was found that air bubbles entrained in the water could be removed by operating in this fashion; much of the air dissolved in the water could be removed by operating with the heater section energized. Experimental measurements were accepted only after visual observation of the water circulating through the test section revealed it to be free of entrained air bubbles.

In establishing the conditions for a test, the water flowrate corresponding to the velocity which when multiplied by the equivalent diameter and divided by the kinematic viscosity would give the specified Reynolds number was set first. Mains water was started flowing in the cooler section and the heater section was energized; the respective controls were set so that the temperature of the water in the system rose at the approximate rate of $1^{o}F$ per minute. The test section power supply was energized and the power generation in the test section was raised incrementally until the specified film temperature difference indicated by the chart recorder was attained. Final adjustments bringing the temperature of the water in the system to equilibrium at the specified value were made by resetting the heater section controls.

When the temperature of the water in the system had attained equilibrium at the value specified for the particular test, five to ten minutes were allowed to elapse in which it was ensured that steady state heat transfer conditions existed in the test section. Then the following measurements were made with the appropriate instruments and recorded:

(1) Temperature of the water upstream of the test section.

(2) Temperature of the water downstream of the test section.

(3) Surface temperatures on the stainless steel tube comprising the effective length.

(4) Stream temperatures upstream and downstream of the effective length.

(5) Flowrate of the water circulating through the system.

(6) Potential drop over the test section length.

(7) Current flowing through the test section.

(8) Pressure differences over the effective length.

(9) System pressure at the pump discharge.

(10) Ambient temperature in the vicinity of the test facility.

The water flowrate was then reset and additional tests were performed in order to demonstrate the effect of flowrate on forced convection heat transfer.

5. DATA ANALYSIS

The results derived from the experimental study are tabulated in Appendix 1. The mannor in which the results were analyzed is outlined in the following sections. The symbols used are defined in Section 8.

5.1 Data Computation

As mentioned previously, local heat transfer coefficients were calculated at the two locations on the inner boundary of the annular passage corresponding to the maximum and minimum separation of the boundaries. The relationship

$$h_c = \frac{(Q/A)}{(T_S - T_B)} \quad \text{B.T.U./hr.ft}^2\ {}^{\circ}\text{F}$$

was used to evaluate the local heat transfer coefficients. The heat flux (Q/A) and the mean film temperature difference $(T_S - T_B)$ were evaluated from measurements of the conditions existing in the region between 12" and 20" from the upstream end of the effective length wherein the heat transfer phenomenon was considered to be representative of fully developed turbulent forced convection heat transfer.

The heat flux (Q/A) was computed from electrical measurements of the heat generation in the test section and/or calorimetric measurements of the heat convection in the water circulating through the test section. The heat flux calculated from electrical measurements was computed by the relationship:

$$\frac{Q}{A} = 3.413\left(\frac{\text{B.T.U.}}{\text{watt-hr.}}\right)\ E\ (\text{volts})\ I\ (\text{amperes})\left(\frac{1}{A_S}\right)\left(\frac{1}{\text{ft}^2}\right)$$

$$= 3.413\ \frac{E\ I}{A_S}\ \text{B.T.U./hr.ft}^2.$$

The heat flux calculated from calorimetric measurements was computed by the relationship

$$\frac{Q}{A} = W\ (\text{lb./hr.})\ C\ (\text{B.T.U./lb.}^\circ\text{F})\ (T_o - T_i)\ (^\circ\text{F})\left(\frac{1}{A_S}\right)\left(\frac{1}{\text{ft}^2}\right)$$

$$= \frac{W\ C}{A_S}\ (T_o - T_i)\ \text{B.T.U./hr.ft}^2.^*$$

The two independent computations of heat flux served to test the validity of the measurements as the experimental results were discarded if the computed values did not agree within approximately $\pm$ 10%.

The mean film temperature difference $(T_S - T_B)$ was obtained by plotting the temperatures measured in the test section as a function of displacement from the upstream end of the effective length. Temperature profiles for the inner surface of the stainless steel tube were formed by drawing smooth curves through the points representing the surface temperature measurements at the locations corresponding to the maximum and minimum separation of the boundaries. The corresponding temperature profiles for the outer surface of the stainless steel tube were formed by drawing smooth curves through points obtained by

---

*The fluid property values used in all the calculations performed were obtained from graphs plotted from the values presented in "Thermodynamic Properties of Steam", by Keenan and Keyes, John Wiley and Sons Incorporated, 1936.

subtracting the temperature drop in the wall from the temperature profiles for the inner surface of the stainless steel tube*. The temperature profile representing the uniform rise of water bulk temperature was formed by joining the points representing the bulk temperatures measured upstream and downstream of the test section by a straight line. Local film temperature differences in the region of fully developed turbulent forced convection heat transfer were evaluated by subtracting the local water bulk temperature from the local outer surface temperature; the mean film temperature difference characterizing the turbulent forced convection heat transfer at the particular location on the inner boundary of the annular passage was obtained by averaging the local film temperature differences.

Moody friction factors were calculated from the average of the measurements of pressure drop over the effective length. The relationship

$$f = (D_e/L)\ (2g/V^2)\ \left(\frac{ft}{sec^2} \times \frac{sec^2}{ft^2}\right)\ (P_i - P_o)\ (\text{ft water})$$

$$= (D_o - D_i)/L\ \ (2g/V^2)\ (P_i - P_o)\ (-)$$

was used to compute the friction factor.

In order to clarify the procedures used in computing the local heat transfer coefficients and friction factors, sample calculations are presented on the following two pages.

*The theory derived for calculating the temperature drop in the wall of the stainless steel tube is presented in Appendix 2.

THE FOLLOWING INFORMATION IS PERTINENT TO THE TEST

DIAMETER RATIO – 2.0 INNER DIAMETER – 0.500" EFFECTIVE
ECCENTRICITY – 29% OUTER DIAMETER – 1.000" LENGTH – 24"
THICKNESS OF WALL OF STAINLESS STEEL TUBE – 0.010"
FLOWRATE – 12.0 U.S. GALLONS/MINUTE
POTENTIAL DROP OVER TEST SECTION – 13.4 VOLTS
CURRENT FLOWING THROUGH TEST SECTION – 265 AMPERES
PRESSURE DIFFERENCE OVER EFFECTIVE LENGTH – 0.78" MERCURY

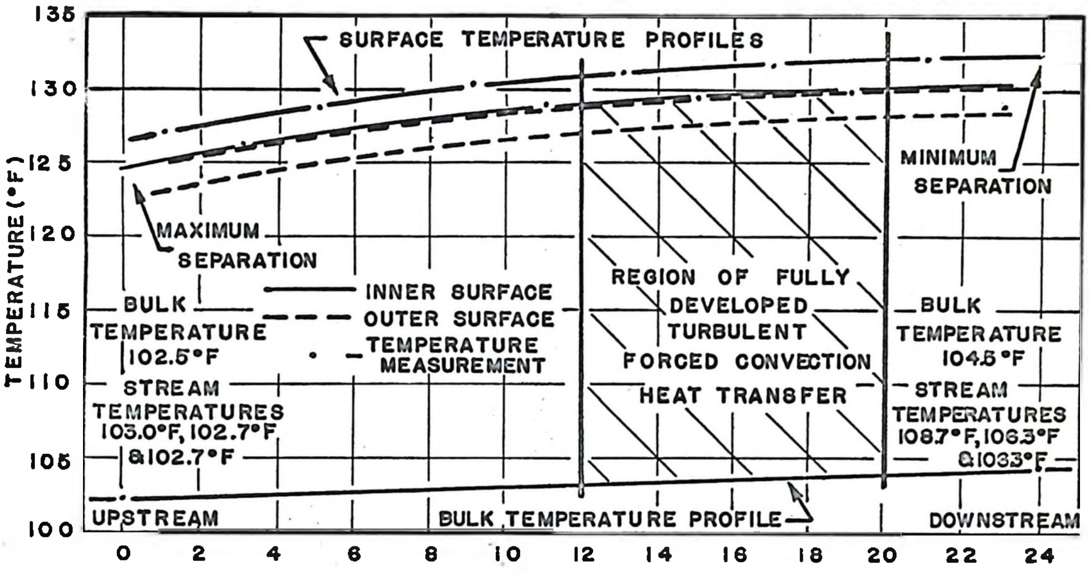

NOTE: AT THE UPSTREAM END OF THE EFFECTIVE LENGTH WHERE HEATING COMMENCES, THE BULK TEMPERATURE & STREAM TEMPERATURES AGREE: AT THE DOWNSTREAM END OF THE EFFECTIVE LENGTH WHERE HEATING CEASES, THE BULK TEMPERATURE & STREAM TEMPERATURES DISAGREE. THE PROBABLE EXPLANATION IS THAT THE WATER IS NOT ADEQUATELY MIXED AT THE LOCATION WHERE THE STREAM TEMPERATURES ARE MEASURED AT THE DOWNSTREAM END OF THE EFFECTIVE LENGTH.

SURFACE AREA NORMAL TO THE FLOW OF HEAT $A_S = \pi \left(\frac{0.5}{12}\right) \text{FT.} \left(\frac{24}{12}\right) \text{FT.} = 0.265 \text{ FT.}^2$

HEAT FLUX CALCULATED FROM ELECTRICAL MEASUREMENTS

$$\frac{Q}{A} = 3.413 \frac{\text{B.T.U.}}{\text{WATT-HR.}} \times 13.4 \text{ VOLTS} \times 265 \text{ AMPERES} \left(\frac{1}{0.265}\right) \frac{1}{\text{FT.}^2} = 45{,}600 \frac{\text{B.T.U.}}{\text{HR.-FT.}^2}$$

HEAT FLUX CALCULATED FROM CALORIMETRIC MEASUREMENTS

$$\frac{Q}{A} = \left(\frac{12.0}{7.48} \times 60\right) \frac{\text{FT.}^3}{\text{HR.}} \times 62.1 \frac{\text{LB.}}{\text{FT.}^3} \times 0.998 \frac{\text{B.T.U.}}{\text{LB.°F}} \times 2.0\text{°F} \left(\frac{1}{0.265}\right) \frac{1}{\text{FT.}^2} = 44{,}800 \frac{\text{B.T.U.}}{\text{HR.-FT.}^2}$$

TEMPERATURE DROP IN THE WALL OF A STAINLESS STEEL TUBE WITH INTERNAL HEAT GENERATION AND ADIABATIC INNER SURFACE

$$\Delta T = \left(\frac{0.25}{12}\right) \text{FT.} \left(\frac{1}{9.7}\right) \frac{\text{HR-FT.}^\circ\text{F}}{\text{B.T.U.}} \left[0.500 - \frac{(0.24)^2}{(0.25)^2-(0.24)^2} \ln\left(\frac{0.25}{0.24}\right)\right] \times 45{,}600 \frac{\text{B.T.U.}}{\text{HR.-FT.}^2} = 1.9^\circ\text{F}$$

CONSEQUENTLY, THE OUTER SURFACE TEMPERATURE PROFILES ARE OBTAINED BY SUBTRACTING 1.9°F FROM EACH OF THE INNER SURFACE TEMPERATURE PROFILES

MAXIMUM SEPARATION	MINIMUM SEPARATION
$(T_S - T_B) = 23.5^\circ F$	$(T_S - T_B) = 25.3^\circ F$
$(T_S - T_B) = 23.6^\circ F$	$(T_S - T_B) = 25.6^\circ F$
$(T_S - T_B) = 23.6^\circ F$	$(T_S - T_B) = 25.6^\circ F$
$(T_S - T_B) = 23.7^\circ F$	$(T_S - T_B) = 25.7^\circ F$
$(T_S - T_B) = 23.8^\circ F$	$(T_S - T_B) = 25.9^\circ F$
$(T_S - T_B)_{MEAN} = 23.7^\circ F$	$(T_S - T_B)_{MEAN} = 25.6^\circ F$

LOCAL H.T. COEFFICIENT

$$h_c = 45{,}600 \frac{\text{B.T.U.}}{\text{HR.-FT.}^2}\left(\frac{1}{23.7}\right)\frac{1}{^\circ\text{F}} = 1930 \frac{\text{B.T.U.}}{\text{HR.-FT.}^2\,^\circ\text{F}}$$

LOCAL H.T. COEFFICIENT

$$h_c = 45{,}600 \frac{\text{B.T.U.}}{\text{HR.-FT.}^2}\left(\frac{1}{25.6}\right)\frac{1}{^\circ\text{F}} = 1785 \frac{\text{B.T.U.}}{\text{HR.-FT.}^2\,^\circ\text{F}}$$

SECTIONAL AREA NORMAL TO THE FLOW OF WATER $A_C = \frac{\pi}{4}\left[\left(\frac{1.00}{12}\right)^2 - \left(\frac{0.50}{12}\right)^2\right] = 0.00409 \text{ FT.}^2$

MEAN WATER VELOCITY IN THE ANNULAR PASSAGE

$$V = \left(\frac{12.0}{7.48 \times 60}\right)\frac{\text{FT.}^3}{\text{SEC.}}\left(\frac{1}{0.00409}\right)\frac{1}{\text{FT.}^2} = 6.55 \frac{\text{FT.}}{\text{SEC.}}$$

EQUIVALENT DIAMETER

$$D_e = (1.00'') - (0.50'') = 0.50''$$

FRICTION FACTOR

$$f = \left(\frac{0.50''}{24''}\right)\left(\frac{2 \times 32.2}{6.55 \times 6.55}\right)\left(\frac{\text{FT.}}{\text{SEC.}^2} \times \frac{\text{SEC.}^2}{\text{FT.}^2}\right) \times 0.78''\text{ MERCURY} \times 1.124 \frac{\text{FT. WATER}}{''\text{ MERCURY}} = 0.0272\ (-)$$

5.2 Data Correlation

Graphical procedures were used to correlate the results of the experimental study. This method of correlation was considered most desirable as the trends resulting from the variation of eccentricity and diameter ratio could be visualized best in a graphical presentation.

In correlating the heat transfer results, a dimensionless heat transfer parameter ($Nu/Pr^{1/3}$) based upon the Nusselt number (Nu) and Prandtl number (Pr) was calculated for each test and plotted on logarithmic paper as a function of the corresponding Reynolds number (Re). This procedure, which assumes that the turbulent forced convection heat transfer is dependent upon $Pr^{1/3}$ was adopted since the actual dependence upon Prandtl number had not been investigated in the experimental study. However, this assumption introduced little error in the analysis of the influence of eccentricity and diameter ratio on turbulent forced convection heat transfer since all tests were performed under nearly the same temperature conditions. As a consequence, the Prandtl number varied little from test to test, and as only relative values were required to assess the trends resulting from the variation of eccentricity and diameter ratio, the Prandtl number variation had insignificant effect upon the final analysis.

The points corresponding to each individual test upon a particular configuration were correlated with a straight line. Examination of the pertinent graphs will reveal a high degree of correlation with a maximum $\pm$ 10% point scatter about the straight line. Figure 5 and Figure 6 illustrate the correlation of the heat transfer results derived from tests upon six concentric configurations and show the influence of diameter ratio upon turbulent forced convection heat transfer in concentric annular passages. The dimensionless parameters used in plotting Figure 5 and Figure 6 were calculated with fluid property values evaluated at the bulk temperature and film temperature respectively. Figure 7, Figure 8, Figure 9 and Figure 10 illustrate the correlation of the heat transfer results derived from tests upon various concentric and eccentric configurations having diameter ratios 1.5, 2.0, 2.5, and 3.0 respectively and show the influence of eccentricity upon turbulent forced convection heat transfer. The dimensionless parameters used in plotting Figure 7, Figure 8, Figure 9 and Figure 10 were calculated with fluid property values evaluated at the bulk temperature.

The influence of eccentricity upon turbulent forced convection heat transfer has been calculated numerically for one Reynolds number value but the correlations presented enable the analysis to be repeated for any other Reynolds number value. In order to assess the influence of eccentricity upon turbulent forced convection heat transfer numerically values of the heat transfer parameter corresponding to each level of eccentricity were evaluated at Reynolds number equal to fifty thousand. These numerical values were ratioed to the numerical value corresponding to concentricity, giving figures of merit indicating the trend resulting from the variation in eccentricity. The analysis was performed for each level of diameter ratio investigated and the figures of merit so derived were plotted as a function of eccentricity. Figure 7, Figure 8, Figure 9 and Figure 10 show the effect of eccentricity upon turbulent forced convection heat transfer corresponding to the particular level of diameter ratio. This information is replotted in Figure 11 where the influence of both eccentricity and diameter ratio upon turbulent forced convection heat transfer is demonstrated.

In order to clarify the procedure used in computing the dimensionless parameters and evaluating the figure of merit, sample calculations are presented on the following page.

In correlating the fluid dynamics results, the friction factor (f) computed from the experimental measurements of each test was plotted on logarithmic paper as a function of Reynolds number (Re). Figure 12 illustrates the correlation between friction factor and Reynolds number for the three concentric configurations investigated. No attempt was made at showing the influence of eccentricity upon friction factor as the results did not warrant so detailed an analysis.

THE FOLLOWING INFORMATION IS PERTINENT TO THE TEST

MEAN BULK TEMPERATURE IN THE REGION OF FULLY DEVELOPED TURBULENT FORCED CONVECTION HEAT TRANSFER

$$T_B = 104.0\,^\circ F$$

THERMAL CONDUCTIVITY

$$K_B = 0.362 \text{ B.T.U./HR.-FT.-}^\circ F$$

KINEMATIC VISCOSITY

$$\nu_B = 0.708 \times 10^{-5} \text{ FT.}^2/\text{SEC.}$$

PRANDTL NUMBER

$$Pr_B = 4.33$$

NUSSELT NUMBER

$$Nu_B = \frac{h_c D_0}{K_B} = \frac{h_c (D_0 - D_i)}{K_B} \left(\frac{\text{B.T.U.}}{\text{HR.-FT.}^2\text{-}^\circ F}\right)(\text{FT.})\left(\frac{\text{HR.-FT.-}^\circ F}{\text{B.T.U.}}\right)$$

MAXIMUM SEPARATION	MINIMUM SEPARATION
$Nu_B = \frac{1930 \times 0.50}{12 \times 0.362} = 222$	$Nu_B = \frac{1785 \times 0.50}{12 \times 0.362} = 206$

HEAT TRANSFER PARAMETER

$$\xi = Nu_B / Pr_B^{1/3}$$

MAXIMUM SEPARATION	MINIMUM SEPARATION
$\xi = 222/1.630 = 136.2$	$\xi = 206/1.630 = 126.4$

REYNOLDS NUMBER

$$Re_B = \frac{V D_e}{\nu_B} = \frac{V(D_0 - D_i)}{\nu_B} = \frac{4}{\pi} \frac{Q}{(D_0^2 - D_i^2)} \times \frac{(D_0 - D_i)}{\nu_B} = \frac{4}{\pi} \frac{Q}{D_0 + D_i} \times \frac{1}{\nu_B}$$

$$\left(\frac{\text{FT.}^3}{\text{SEC.}}\right)\left(\frac{1}{\text{FT.}} \times \frac{\text{SEC.}}{\text{FT.}^2}\right) = \frac{4}{\pi}\left(\frac{12.0}{7.48 \times 60} \times \frac{12}{1.00 + 0.50}\right)\left(\frac{10^5}{0.708}\right) = 38{,}400$$

HEAT TRANSFER PARAMETER CORRESPONDING TO CONCENTRICITY

$$\xi_0 = 132.0$$

FIGURE OF MERIT

$$\xi/\xi_0 = \text{RATIO}\left(\frac{Nu}{Nu_0}\right)\left(\frac{Pr_0^{1/3}}{Pr^{1/3}}\right)$$

MAXIMUM SEPARATION	MINIMUM SEPARATION
RATIO = 136.2/132.0 = 1.032	RATIO = 126.4/132.0 = 0.955

6. DISCUSSION

6.1 Accuracy of Results

This section concerns the analysis of error in the correlation of the experimental results. In performing the analysis, the maximum possible error involved in each measurement was used. As a consequence, the uncertainty in the correlation of the experimental results indicated by the analysis represents the maximum error resulting from the improbable combination of the maximum values of the individual errors. It is understood that the probable error is much smaller by a considerable factor.

The fluid property values used in calculating the dimensionless parameters were assumed to be those for pure water. Although small errors are undoubtedly involved in using these fluid property values, only the error associated with reading the numerical value of the fluid property from a graph has been considered in the error analysis.

The results of the error analysis which is presented in tabular form on the following two pages, indicate that the uncertainty in the correlation of the heat transfer results could be as great as $\pm$ 21.5% and that the uncertainty in the correlation of the fluid dynamics results could be as great as $\pm$ 49.5%, mainly as a result of the large possible error involved in the calculation of equivalent diameter.

#	DESCRIPTION OF ERROR	MAXIMUM PERCENT ERROR	MAXIMUM ABSOLUTE ERROR
	(HEAT FLUX) = 3.413 (VOLTAGE MEASUREMENT)(CURRENT MEASUREMENT) X ($\frac{1}{\text{AREA}}$)		
1.	VOLTAGE MEASUREMENT		
	-INSTRUMENT ERROR AT 1/2 SCALE	±2.0%	
	-VOLTAGE FLUCTUATIONS	±1.0%	
2.	CURRENT MEASUREMENT		
	-INSTRUMENT ERROR AT 1/2 SCALE	±2.0%	
	-CURRENT FLUCTUATIONS	± 1.0%	
3.	AREA = π (DIAMETER)(LENGTH)		
	-DIAMETER 0.500" ± 0.0025"	± 0.5%	
	-LENGTH 24" ± 0.125"	± 0.5%	
	ERROR IN HEAT FLUX CALCULATION	± 6.0%	
	(FILM TEMPERATURE DIFFERENCE) = (INNER SURFACE TEMPERATURE) - (WALL TEMPERATURE DROP) - (BULK FLUID TEMPERATURE)		
1.	INNER SURFACE TEMPERATURE		
	- THERMOELECTRIC ERROR IN 130°F		± 1.0°F
	- RECORDER INACCURACY		± 0.3°F
2.	WALL TEMPERATURE DROP		
	-ESTIMATED INACCURACY		± 0.1°F
3.	BULK FLUID TEMPERATURE		
	- THERMOMETER ERROR		±0.1°F
	ERROR IN FILM TEMPERATURE DIFFERENCE		± 1.5°F
	ERROR IN 30°F TEMPERATURE DIFFERENCE	± 5.0%	
	(NUSSELT NUMBER) = (HEAT TRANSFER COEFFICIENT)($\frac{\text{EQUIVALENT DIAMETER}}{\text{THERMAL CONDUCTIVITY}}$)		
1.	HEAT TRANSFER COEFFICIENT		
	- HEAT FLUX	±6.0%	
	- FILM TEMPERATURE DIFFERENCE	±5.0%	
2.	EQUIVALENT DIAMETER = OUTER DIAMETER - INNER DIAMETER		
	-OUTER DIAMETER		±0.0150"
	-INNER DIAMETER		±0.0025"
	-ERROR IN 0.750"-0.500"	±7.5%	
3.	THERMAL CONDUCTIVITY		
	-READING ERROR ±0.5%	±0.5%	
	ERROR IN NUSSELT NUMBER CALCULATION	±19.0%	
	(HEAT TRANSFER PARAMETER) = (NUSSELT NUMBER)(PRANDTL NUMBER)$^{-1/3}$		
1.	NUSSELT NUMBER		
	-CALCULATION ERROR	±19.0%	
2.	(PRANDTL NUMBER)$^{-1/3}$		
	- READING ERROR ±3.0%	± 1.0%	
	ERROR IN HEAT TRANSFER PARAMETER	±20.0%	

#	DESCRIPTION OF ERROR	MAXIMUM PERCENT ERROR	MAXIMUM ABSOLUTE ERROR
	$\left(\text{FRICTION FACTOR}\right) = 2g\left(\dfrac{\text{EQUIVALENT DIAMETER}}{\text{LENGTH}}\right) \times \left(\dfrac{\text{PRESSURE DIFFERENCE}}{\text{VELOCITY}^2}\right)$		
1.	EQUIVALENT DIAMETER = OUTER DIAMETER − INNER DIAMETER		
	− OUTER DIAMETER		±0.0150"
	− INNER DIAMETER		±0.0025"
	− ERROR IN 0.750" − 0.500"	±7.5%	
2.	LENGTH		
	− ERROR IN 24" ±0.125"	±0.5%	
3.	PRESSURE DIFFERENCE		
	− INSTRUMENT ERROR	±10.0%	
	− PRESSURE DIFFERENCE FLUCTUATIONS	± 1.0%	
4.	$\text{VELOCITY} = \dfrac{4}{\pi}\left[\dfrac{\text{VOLUMETRIC FLOWRATE}}{\left(\text{OUTER DIAM.} + \text{INNER DIAM.}\right)\left(\text{OUTER DIAM.} - \text{INNER DIAM.}\right)}\right]$		
	− VOLUMETRIC FLOWRATE ± 6.0%		
	− OUTER DIAM. + INNER DIAM. ± 1.5%		
	− OUTER DIAM. − INNER DIAM. ± 7.5%		
	− ERROR IN VELOCITY ± 15.0%		
	− ERROR IN VELOCITY ^{2}	±30.0%	
	ERROR IN FRICTION FACTOR CALCULATION	±49.0%	
	$\left(\text{REYNOLDS NUMBER}\right) = \dfrac{4}{\pi}\left(\dfrac{\text{VOLUMETRIC FLOWRATE}}{\text{OUTER DIAM.} + \text{INNER DIAM.}}\right) \times \left(\dfrac{1}{\text{KINEMATIC VISCOSITY}}\right)$		
1.	VOLUMETRIC FLOWRATE		
	− INSTRUMENT ERROR	±5.0%	
	− FLOWRATE FLUCTUATIONS	±1.0%	
2.	OUTER DIAM. + INNER DIAM.		
	− OUTER DIAMETER		±0.0150"
	− INNER DIAMETER		±0.0025"
	− ERROR IN 0.750" + 0.500"	±1.5%	
3.	KINEMATIC VISCOSITY		
	− READING ERROR ±0.5%	±0.5%	
	ERROR IN REYNOLDS NUMBER CALCULATION	±8.0%	

$$\left[\begin{matrix}\text{UNCERTAINTY IN}\\ \text{CORRELATION OF}\\ \text{H.T. RESULTS}\end{matrix}\right] = \sqrt{\left[\begin{matrix}\text{ERROR IN}\\ \text{H.T. PARAMETER}\\ \text{CALCULATION}\end{matrix}\right]^2 + \left[\begin{matrix}\text{ERROR IN}\\ \text{REYNOLDS NO.}\\ \text{CALCULATION}\end{matrix}\right]^2} = \sqrt{(\pm 20.0\%)^2 + (\pm 8.0\%)^2} = \pm 21.5\%$$

$$\left[\begin{matrix}\text{UNCERTAINTY IN}\\ \text{CORRELATION OF}\\ \text{F.D. RESULTS}\end{matrix}\right] = \sqrt{\left[\begin{matrix}\text{ERROR IN}\\ \text{FRICTION FACTOR}\\ \text{CALCULATION}\end{matrix}\right]^2 + \left[\begin{matrix}\text{ERROR IN}\\ \text{REYNOLDS NO.}\\ \text{CALCULATION}\end{matrix}\right]^2} = \sqrt{(\pm 49.0\%)^2 + (\pm 8.0\%)^2} = \pm 49.5\%$$

Although these large uncertainties cast suspicion upon the validity of the correlations presented, it must be emphasized that these are extreme values which could only result from the improbable combination of the maximum values of the individual errors in connection with tests upon one particular annular test configuration. When considered in this manner, it would appear that the uncertainties in the correlations of most of the experimental results are no greater than those associated with any comparable experimental study.

6.2 Heat Transfer in Concentric Annular Passages

The results presented in Figure 5 and Figure 6 showing the influence of diameter ratio upon turbulent forced convection heat transfer in concentric annular passages are not in complete agreement with the results predicted by the correlations derived by Monrad and Pelton and Stein and Begell. The results presented appear to be dependent upon diameter ratio raised to the 1/4 power rather than diameter ratio raised to the 1/2 power as suggested by both Monrad and Pelton and Stein and Begell. However, the experimental evidence supporting this functional relationship is insufficient to justify another correlation for turbulent forced convection heat transfer in concentric annular passages.

In fairness to the results presented, it must be noted that the annular test configurations investigated in the experimental study were not identical dimensionally to the annular test configurations investigated by Monrad and Pelton and Stein and Begell. As it would seem unreasonable to expect similar heat transfer phenomena to occur in annular passages of the same diameterratio but different dimensions, it is possible that the results of the experimental study are consistent with the correlations derived by Monrad and Pelton and Stein and Begell. Further investigation is required to resolve this point.

6.3 Heat Transfer in Eccentric Annular Passages

The results presented in Figure 7, Figure 8, Figure 9 and Figure 10 showing the influence of eccentricity upon turbulent forced convection heat transfer in eccentric annular passages are in general agreement with the results presented by Diskind and Faure. The results presented indicate that eccentricity and diameter ratio have a definite effect upon the heat transfer phenomenon and that the heat transfer from the two locations on the inner boundary of the annular passage is affected differently. Increasing eccentricity causes the heat transfer to increase at the location corresponding to the maximum separation of the inner and outer boundaries of the annular passage and to decrease at the location corresponding to the minimum separation of the inner and outer boundaries of the annular passage. Assuming a continuous variation in heat transfer around the inner boundary of the annular passage, it must be concluded that the average heat transfer decreases since the decrease in heat transfer in the vicinity of the location corresponding to the minimum separation of the boundaries is greater than the increase in heat transfer in the vicinity of the location corresponding to the maximum separation of the boundaries.

The results presented in Figure 11 showing the influence of diameter ratio upon turbulent forced convection heat transfer in eccentric annular passages are in general agreement with the results presented by Fauré. At a particular level of eccentricity, the heat transfer varies in inverse proportion to the diameter ratio; the greater variations occur at the smaller diameter ratios. Ranges in which eccentricity does not influence heat transfer are found in connection with the larger diameter ratios.

The apparent explanation of the influence of eccentricity and diameter ratio upon turbulent forced convection heat transfer has been suggested by Fauré. From a study of temperature profiles in eccentric annular passages, Fauré was able to show that the heat transfer phenomenon was only affected by eccentricity and/or diameter ratio when the normal development of the thermal boundary layer at the inner boundary of the annular passage was disturbed by the presence of the outer boundary of the annular passage. It appears then, that the influence of eccentricity and diameter ratio upon turbulent forced convection heat transfer is derived from the development of a thermal boundary layer on the inner boundary of the annular passage. The fact that in certain annular passages, ranges in which eccentricity did not influence heat transfer were found is explained by postulating that the normal development of the thermal boundary layer was not disturbed until these ranges of eccentricity were exceeded. A mathematical solution of turbulent forced convection heat transfer in eccentric annular passages using boundary layer theory is required in order to verify this apparent explanation.

6.4 Fluid Dynamics in Concentric Annular Passages

The results presented in Figure 12 showing the influence of diameter ratio upon friction factors for turbulent flow in concentric annular passages are in excellent agreement with the results presented by Diskind. The results presented indicate that the friction factors pertaining to the different levels of diameter ratio can be correlated satisfactorily by a single straight line which approximately represents the variation of friction factor with Reynolds number for flow in a tube with 0.0005 relative roughness. It would appear that the friction factors for turbulent flow in concentric annular passages can be satisfactorily predicted from published friction factors for turbulent flow in tubes.

7. CONCLUSIONS

An experimental study of turbulent forced convection heat transfer to water flowing in nineteen different annular test configurations has resulted in graphical correlations showing the influence of eccentricity and/or diameter ratio upon the heat transfer phenomenon occurring at the two locations on the inner boundary of the annular passage corresponding to the maximum and minimum separation of the inner and outer boundaries. The correlations derived generally confirm the results obtained by other investigators and extend the range of diameter ratios investigated. The results pertaining to heat transfer in concentric annular passages are not in complete agreement with the results predicted by the correlations derived by Monrad and Pelton and Stein and Begell in that the functional relationship between heat transfer and diameter ratio appears to be different than that predicted. The results pertaining to heat transfer in eccentric annular passages are in general agreement with the results published by Diskind and Fauré with respect to the influence of eccentricity and diameter ratio upon heat transfer.

An experimental study of the fluid dynamics of water flowing in three different annular test configurations has resulted in a graphical correlation showing the influence of diameter ratio upon friction factors for turbulent flow in concentric annular passages. The correlation derived indicates that the friction factors for turbulent flow in concentric annular passages can be satisfactorily predicted from published friction factors for turbulent flow in tubes.

8. NOMENCLATURE

Arabic Symbols	Description	Units
A	Area	ft^2
A_S	Surface area	ft^2
A_C	Cross section area	ft^2
C	Specific heat	B.T.U./lb^{o}F
D	Diameter	ft
D_e	Equivalent diameter	
	$(D_e = 4 \frac{\text{Cross Section Area}}{\text{Wetted Perimeter}} = D_o - D_i)$	ft
D_i	Inner diameter of annular passage	ft
D_o	Outer diameter of annular passage	ft
D_o/D_i	Diameter ratio $(D_o/D_i = 2\ R_o/2\ R_i)$	-
E	Potential drop over test section	volts
f	Moody friction factor	-
g	Gravitational acceleration constant	ft./sec.^{2}
h_c	Convective heat transfer coefficient	B.T.U./hr.ft^2 ^{o}F
I	Current flowing through test section	amperes
k	Thermal conductivity	B.T.U./hr.ft^{o}F
L	Effective length	ft
P	Pressure	ft. water
P_i	Pressure upstream of effective length	ft. water

P_o	Pressure downstream of effective length	ft. water
P_i-P_o	Pressure drop over effective length	ft. water
Q	Volumetric flowrate	U.S. gallons per minute
Q	Heat generation	B.T.U./hr.
Q'	Heat generation per unit length	B.T.U./hr.ft.
Q"	Heat generation per unit area	B.T.U./hr.ft^2
Q"'	Heat generation per unit volume	B.T.U./hr.ft^3
r	Radius	ft
r_i	Inner radius of tube	ft
r_o	Outer radius of tube	ft
R_i	Inner radius of annular passage	ft
R_o	Outer radius of annular passage	ft
s	Length of shorter support leg	ft
S	Length of longer support leg	ft
T	Temperature	^oF
T_B	Bulk temperature	^oF
T_i	Bulk temperature at test section inlet	^oF
T_o	Bulk temperature at test section outlet	^oF
T_S	Surface temperature	^oF
T_o-T_i	Bulk temperature rise	^oF
T_S-T_B	Film temperature difference	^oF
ΔT	Temperature drop in wall of tube	^oF
U	Overall heat transfer coefficient	B.T.U./hr.ft^2 ^oF
V	Mean flow velocity	ft/sec.
W	Mass flowrate	lb/hr.

Greek Symbols	Description	Units
α	Angle	-
β	Angle	-
γ	Angle	-
δ	Separation of axes	ft
ε	Eccentricity ($\varepsilon = \frac{\delta}{R_o - R_i}$)	-
ζ	Heat transfer parameter ($\zeta = \frac{Nu}{Pr^{1/3}}$)	-
η	Heat exchanger effectiveness	-
λ	Constant of integration	-
μ	Dynamic viscosity	lb/ft.sec.
ν	Kinematic viscosity	ft^2/sec

Dimensionless Parameters	Description	Units
Nu	Nusselt number ($Nu = \frac{h_c D_e}{k}$)	-
Pr	Prandtl number ($Pr = \frac{\mu C_p}{k}$)	-
Re	Reynolds number ($Re = \frac{V D_e}{\nu}$)	-
St	Stanton number ($St = \frac{h_c}{\rho C V}$)	-

Letter Subscripts	Description	Units
B	Bulk temperature	-
F	Film temperature	-
C	Cross section	-
S	Surface	-
S.S.	Stainless steel	-
i	Inner or inlet	-
o	Outer or outlet	-

9. REFERENCES

1. A. S. Foust and G. A. Christian, "Non-Boiling Heat Transfer in Annuli", A.I.Ch.E. Transactions, Volume 36, (541-554), 1940.

2. C. C. Monrad and J. F. Pelton, "Heat Transfer by Convection in Annular Spaces", A.I.Ch.E. Transactions, Volume 38, (593-611), 1942.

3. F. G. Carpenter, A. P. Colburn, E. M. Schoenburn and A. Wurster, "Heat Transfer and Friction of Water in an Annular Space", A.I.Ch.E. Transactions, Volume 42, (165-187), 1946.

4. R. P. Stein and W. Begell, "Heat Transfer to Water in Turbulent Flow in Internally Heated Annuli", A.I.Ch.E. Journal, Volume 4, (127-131), 1958.

5. R. G. Deissler and M. F. Taylor, "Analysis of Fully Developed Turbulent Heat Transfer and Flow in an Annulus with Various Eccentricities", N.A.C.A.-TN-3451, March 16, 1955.

6. J. F. Heyda, "Heat Transfer in Turbulent Flow Through Non-Concentric Annuli Having Unequal Heat Release from the Walls", A.P.E.X.-391, June 1957.

7. T. Diskind, "Heat Transfer and Pressure Drop in Eccentric Annuli", N.Y.O.-9649, September 30, 1961.

8. J. Fauré, "Étude de la Convection Forcée", Annales de Physique, Novembre-Décembre, 1960.

9. R. L. Judd, "English Translation of Étude de la Convection Forcée", McMaster University, April 1962.

10. ILLUSTRATIONS

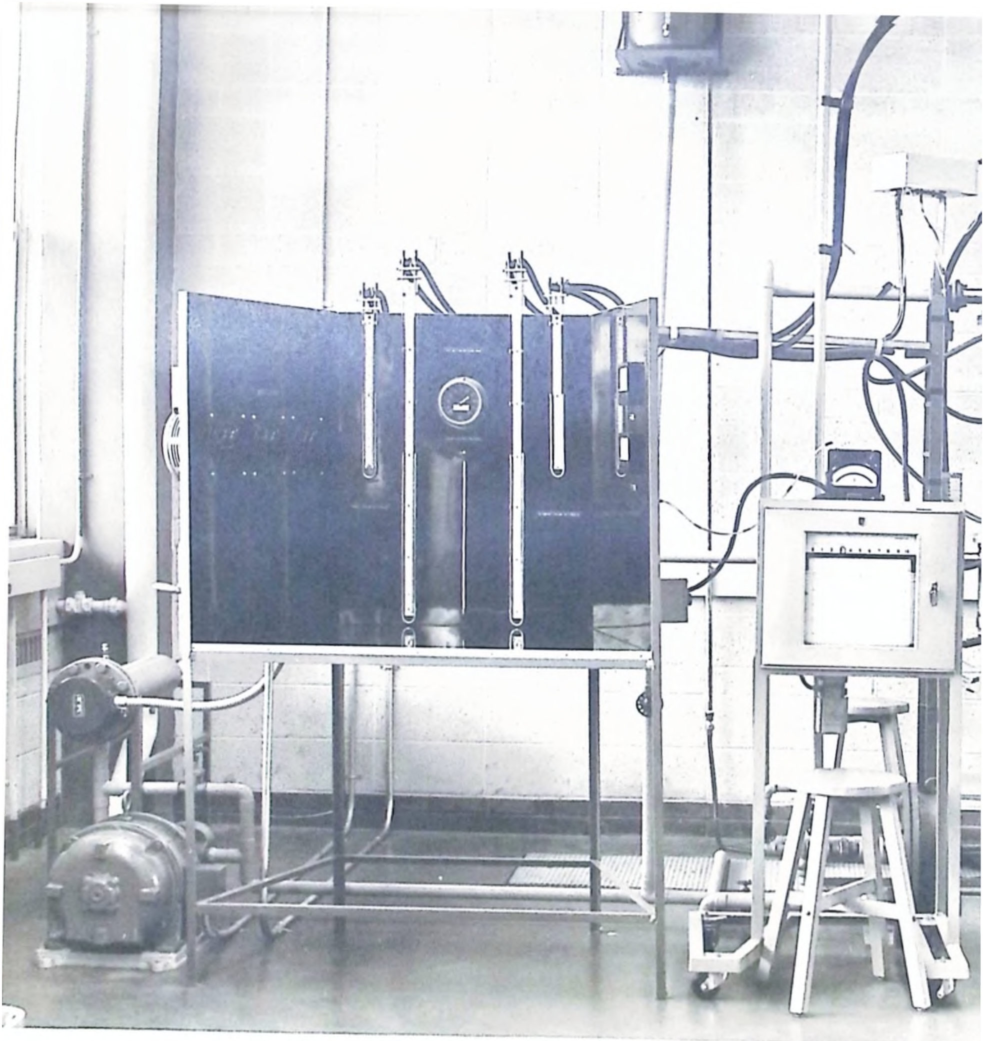

TEST FACILITY

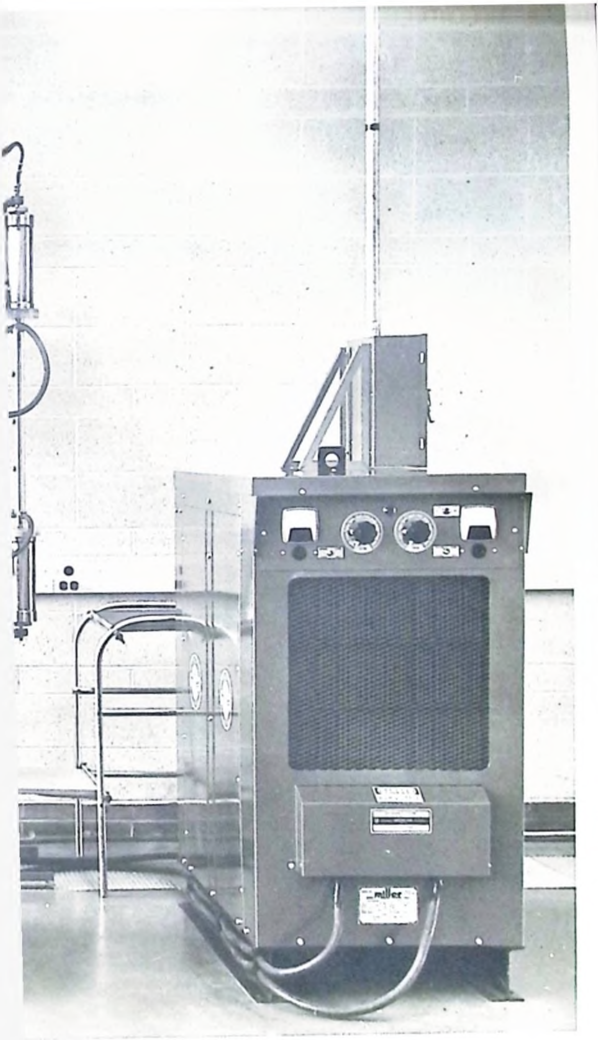

FIGURE # 1.

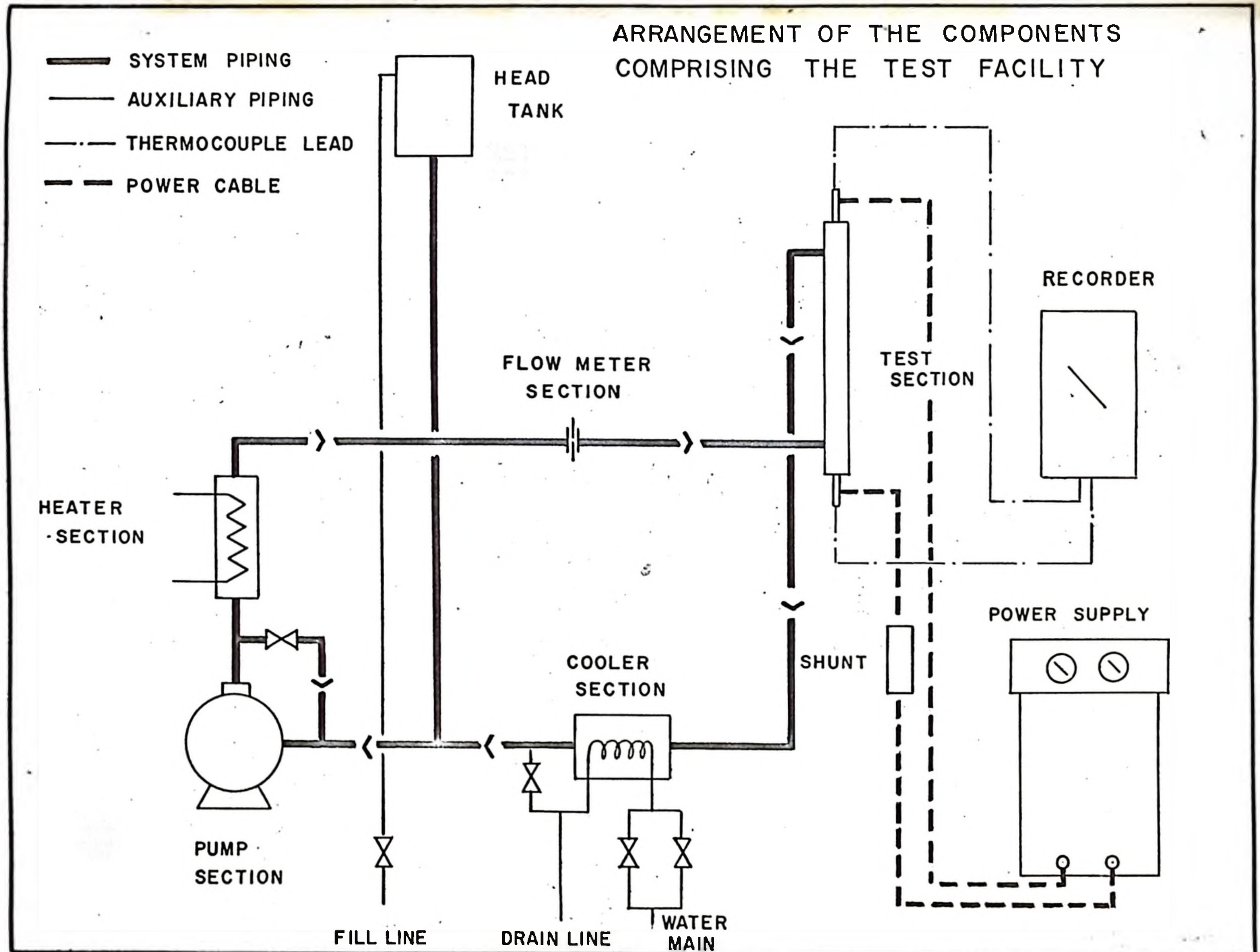
ARRANGEMENT OF THE COMPONENTS
COMPRISING THE TEST FACILITY
SYSTEM PIPING
AUXILIARY PIPING
THERMOCOUPLE LEAD
POWER CABLE
HEAD
TANK
RECORDER
FLOW METER
SECTION
TEST
SECTION
HEATER
SECTION
POWER SUPPLY
COOLER
SECTION
SHUNT
PUMP
SECTION
FILL LINE
DRAIN LINE
WATER
MAIN

FIGURE # 2

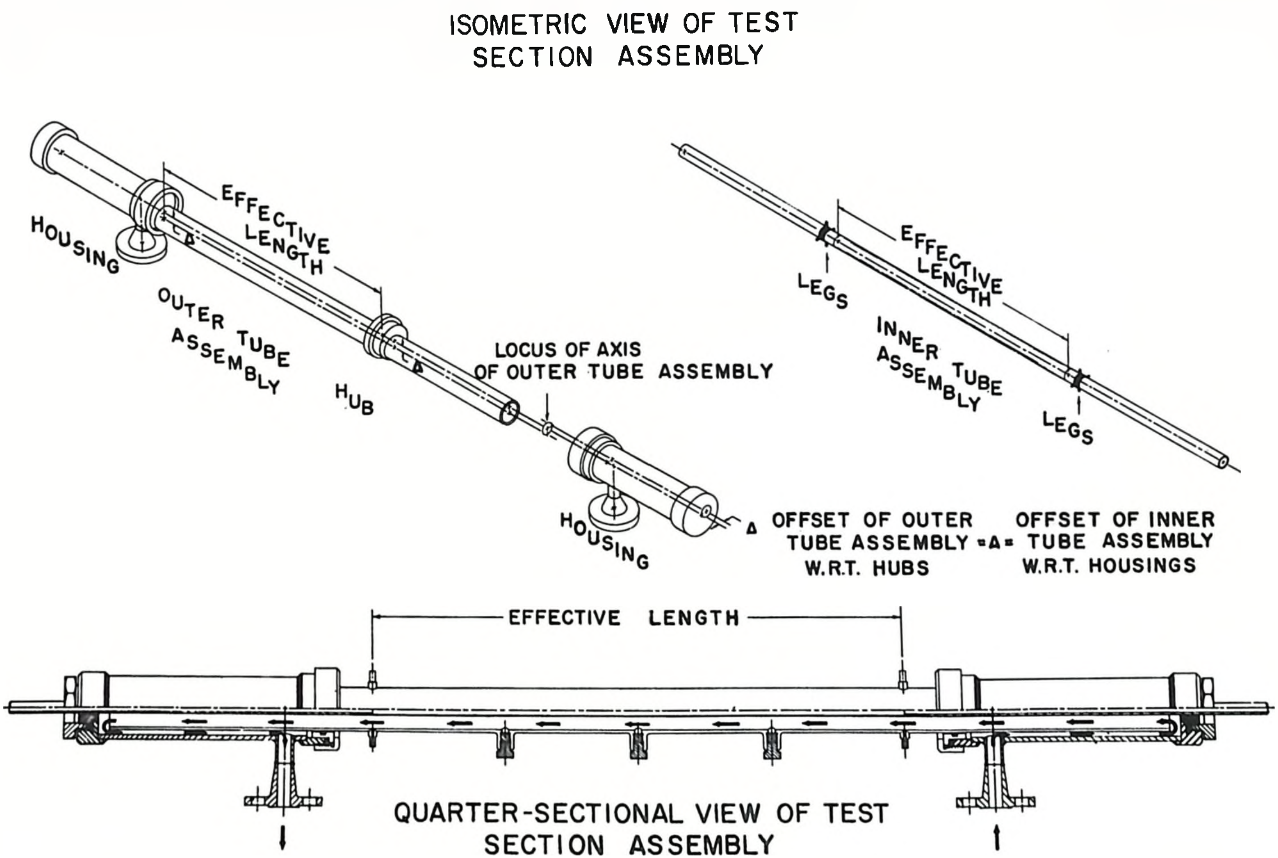
ISOMETRIC VIEW OF TEST SECTION ASSEMBLY
HOUSING
EFFECTIVE LENGTH
OUTER TUBE ASSEMBLY
HUB
LOCUS OF AXIS OF OUTER TUBE ASSEMBLY
HOUSING
EFFECTIVE LENGTH
LEGS
INNER TUBE ASSEMBLY
LEGS
Δ OFFSET OF OUTER TUBE ASSEMBLY W.R.T. HUBS = Δ = OFFSET OF INNER TUBE ASSEMBLY W.R.T. HOUSINGS
EFFECTIVE LENGTH
QUARTER-SECTIONAL VIEW OF TEST SECTION ASSEMBLY

FIGURE # 3.

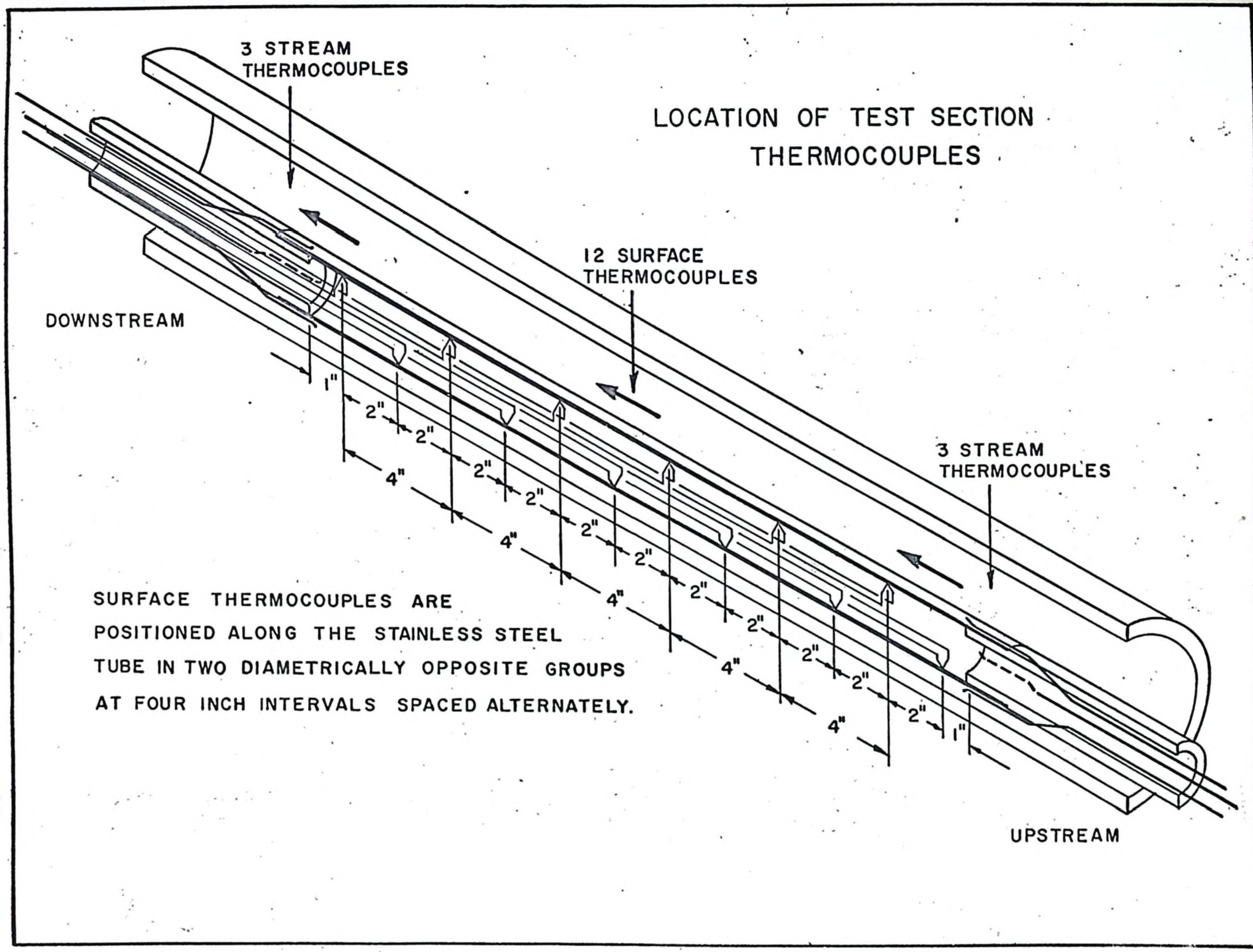
3 STREAM THERMOCOUPLES
LOCATION OF TEST SECTION THERMOCOUPLES
12 SURFACE THERMOCOUPLES
DOWNSTREAM
1"
2"
4"
3 STREAM THERMOCOUPLES
SURFACE THERMOCOUPLES ARE POSITIONED ALONG THE STAINLESS STEEL TUBE IN TWO DIAMETRICALLY OPPOSITE GROUPS AT FOUR INCH INTERVALS SPACED ALTERNATELY.
UPSTREAM

FIGURE # 4

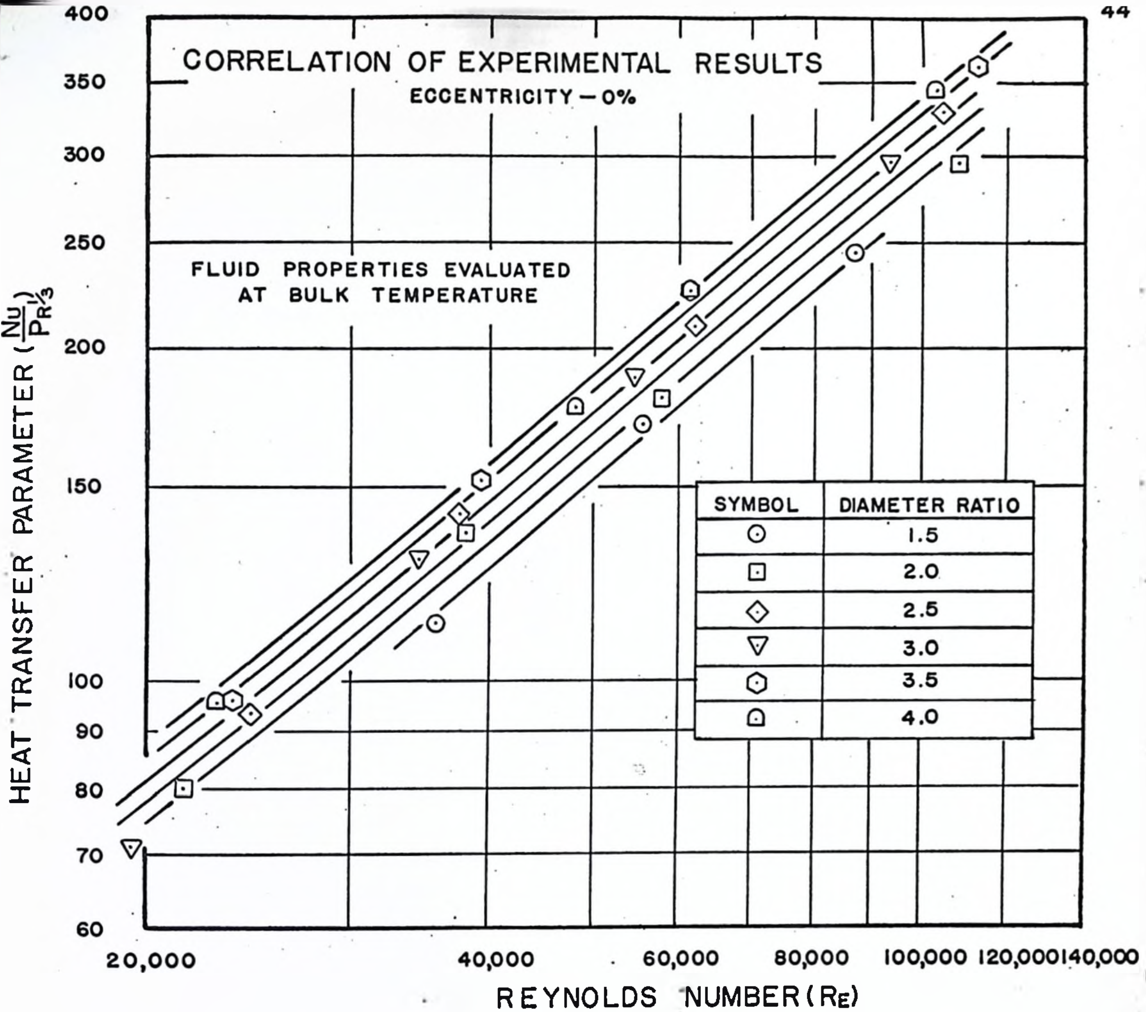
CORRELATION OF EXPERIMENTAL RESULTS
ECCENTRICITY — 0%
FLUID PROPERTIES EVALUATED AT BULK TEMPERATURE
HEAT TRANSFER PARAMETER ($\frac{Nu}{Pr^{1/3}}$)
REYNOLDS NUMBER (RE)
400
350
300
250
200
150
100
90
80
70
60
20,000
40,000
60,000
80,000
100,000
120,000
140,000
SYMBOL
DIAMETER RATIO
1.5
2.0
2.5
3.0
3.5
4.0

FIGURE # 5

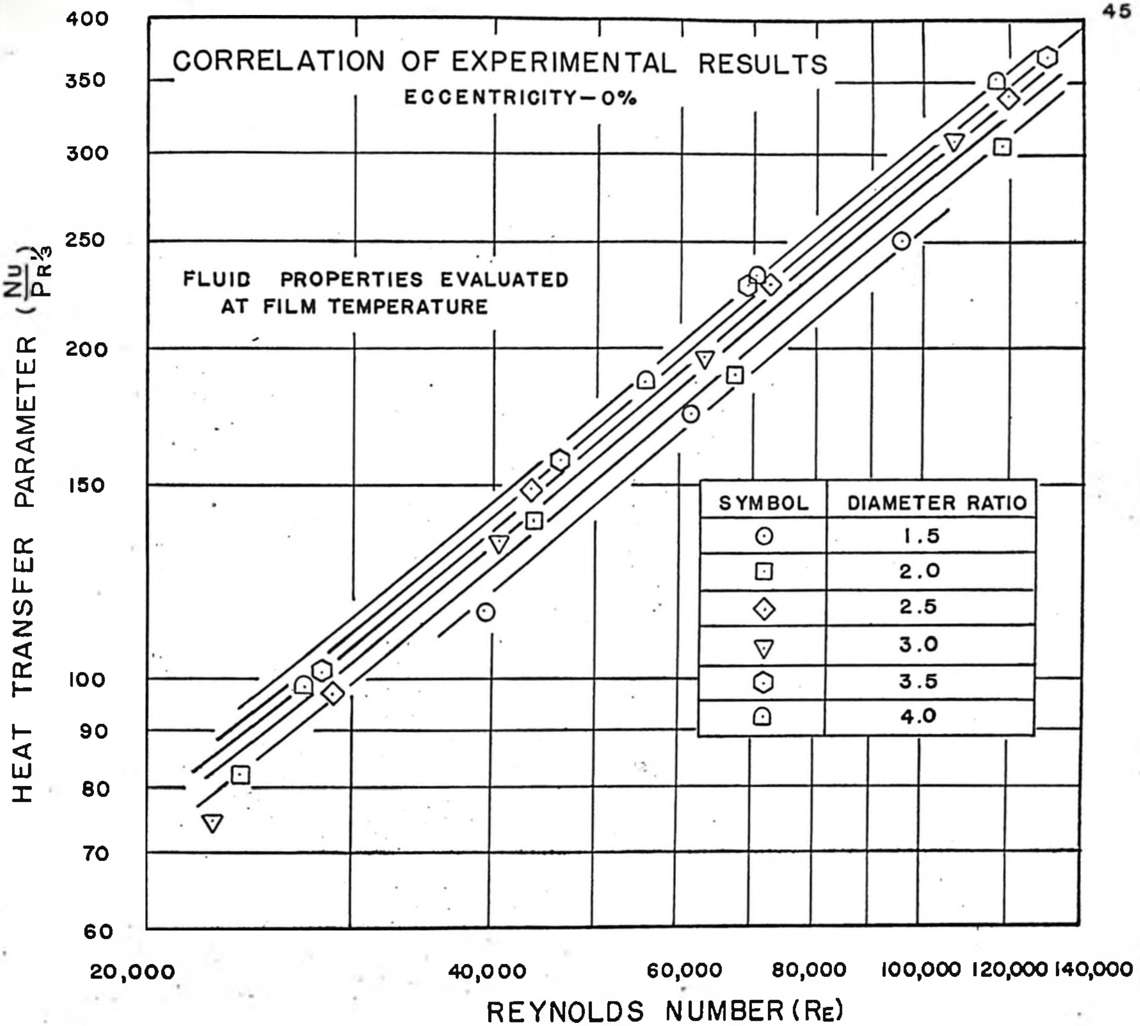
CORRELATION OF EXPERIMENTAL RESULTS
ECCENTRICITY—0%
FLUID PROPERTIES EVALUATED AT FILM TEMPERATURE
SYMBOL
DIAMETER RATIO
1.5
2.0
2.5
3.0
3.5
4.0
HEAT TRANSFER PARAMETER $\left(\frac{Nu}{Pr^{1/3}}\right)$
400
350
300
250
200
150
100
90
80
70
60
20,000
40,000
60,000
80,000
100,000
120,000
140,000
REYNOLDS NUMBER (Re)

FIGURE # 6

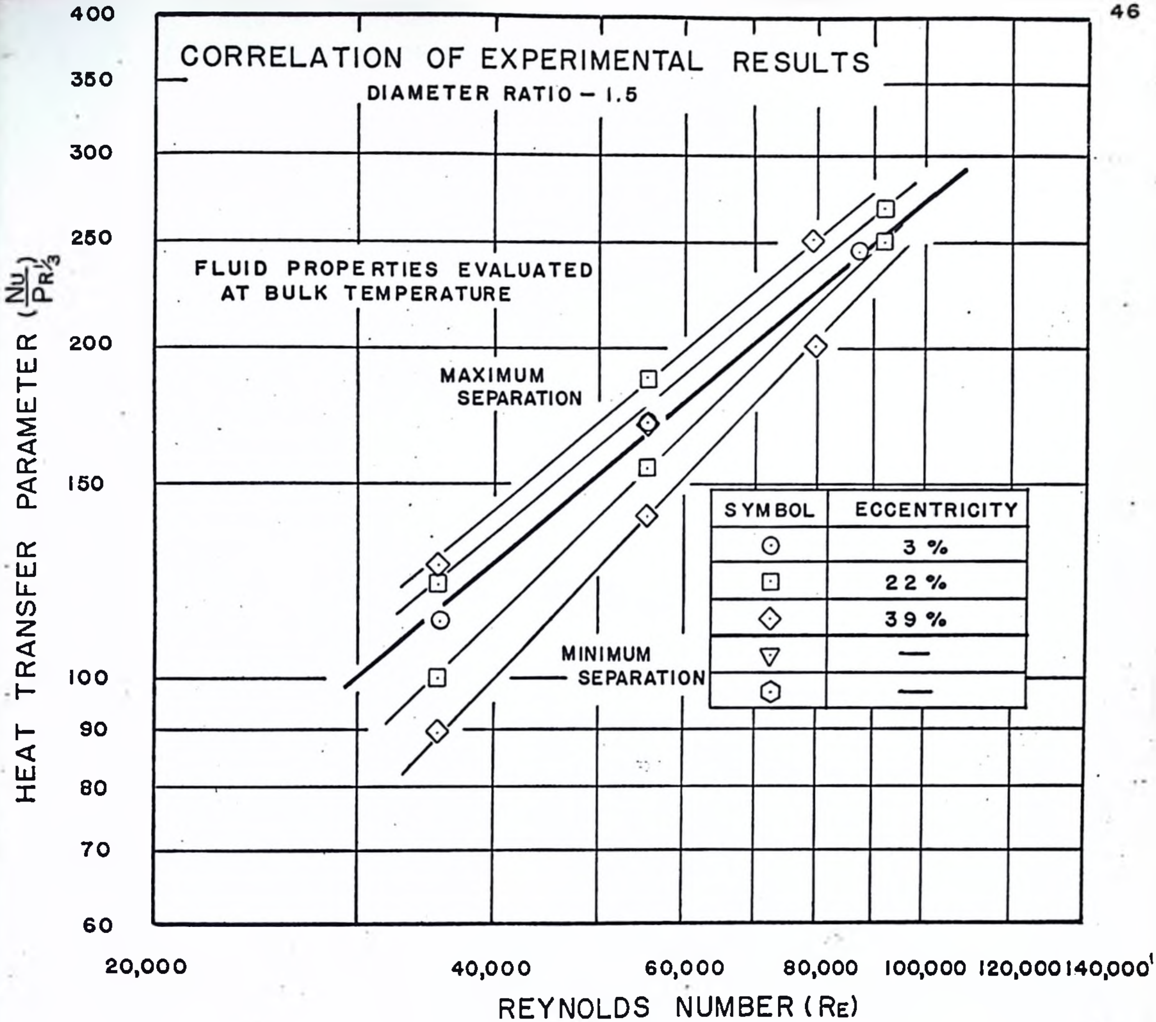
CORRELATION OF EXPERIMENTAL RESULTS
DIAMETER RATIO – 1.5
FLUID PROPERTIES EVALUATED AT BULK TEMPERATURE
MAXIMUM SEPARATION
MINIMUM SEPARATION
HEAT TRANSFER PARAMETER ($\frac{Nu}{Pr^{1/3}}$)
REYNOLDS NUMBER (RE)
400
350
300
250
200
150
100
90
80
70
60
20,000
40,000
60,000
80,000
100,000
120,000
140,000
SYMBOL | ECCENTRICITY
⊙ | 3 %
⊡ | 22 %
◇ | 39 %
▽ | —
⬡ | —

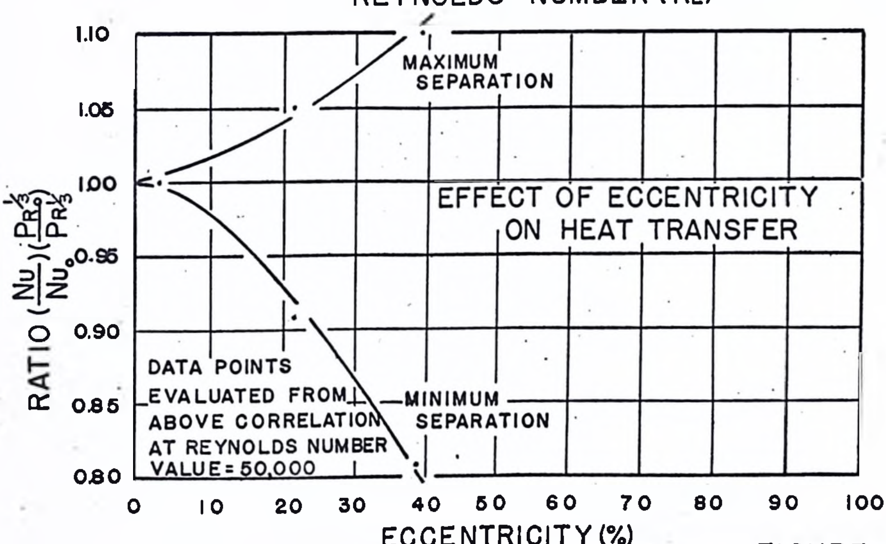
EFFECT OF ECCENTRICITY ON HEAT TRANSFER
MAXIMUM SEPARATION
MINIMUM SEPARATION
DATA POINTS EVALUATED FROM ABOVE CORRELATION AT REYNOLDS NUMBER VALUE = 50,000
RATIO ($\frac{Nu}{Nu_0}$)($\frac{Pr_0^{1/3}}{Pr^{1/3}}$)
ECCENTRICITY (%)
1.10
1.05
1.00
0.95
0.90
0.85
0.80
0
10
20
30
40
50
60
70
80
90
100

FIGURE #7

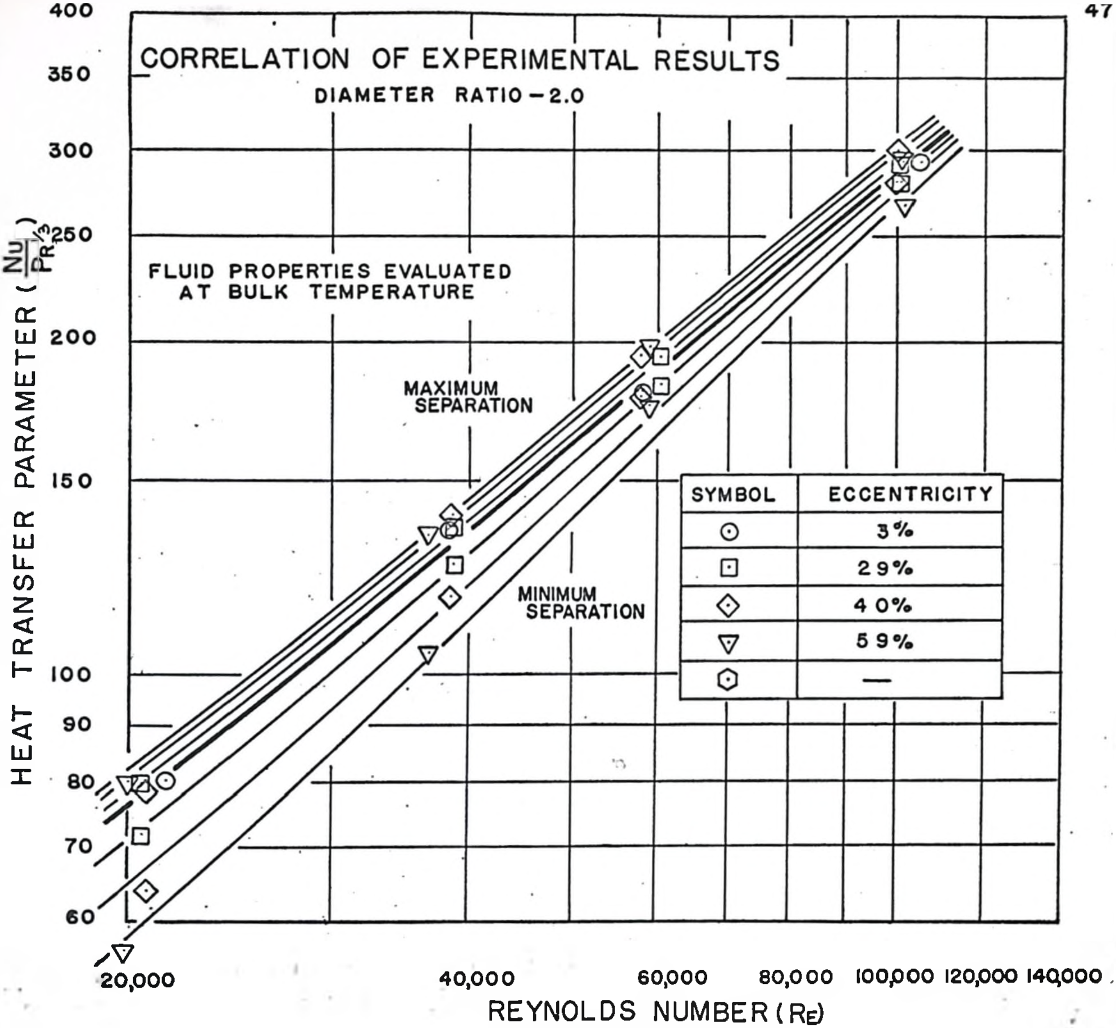
CORRELATION OF EXPERIMENTAL RESULTS
DIAMETER RATIO – 2.0
FLUID PROPERTIES EVALUATED AT BULK TEMPERATURE
MAXIMUM SEPARATION
MINIMUM SEPARATION
SYMBOL
ECCENTRICITY
3%
29%
40%
59%
—
HEAT TRANSFER PARAMETER ($\frac{Nu}{Pr^{1/3}}$)
400
350
300
250
200
150
100
90
80
70
60
20,000
40,000
60,000
80,000
100,000
120,000
140,000
REYNOLDS NUMBER (R_E)

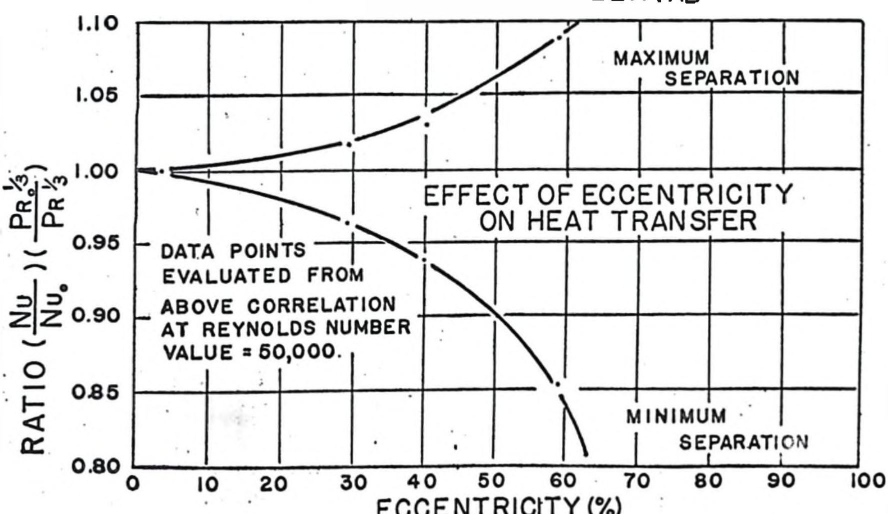
EFFECT OF ECCENTRICITY ON HEAT TRANSFER
MAXIMUM SEPARATION
MINIMUM SEPARATION
DATA POINTS EVALUATED FROM ABOVE CORRELATION AT REYNOLDS NUMBER VALUE = 50,000.
RATIO ($\frac{Nu}{Nu_o}$)($\frac{Pr_o^{1/3}}{Pr^{1/3}}$)
1.10
1.05
1.00
0.95
0.90
0.85
0.80
0
10
20
30
40
50
60
70
80
90
100
ECCENTRICITY (%)

FIGURE # 8

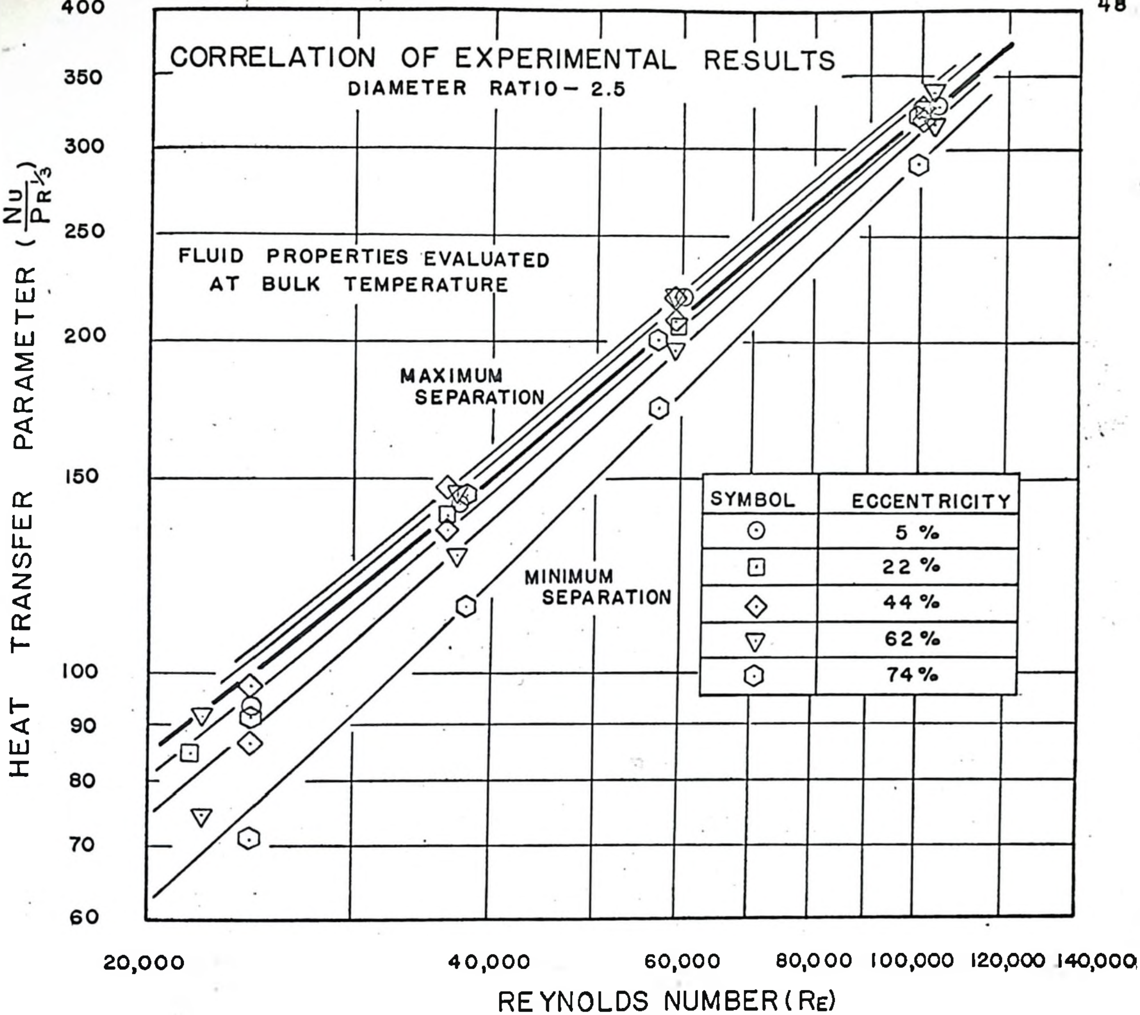
CORRELATION OF EXPERIMENTAL RESULTS
DIAMETER RATIO – 2.5
FLUID PROPERTIES EVALUATED AT BULK TEMPERATURE
MAXIMUM SEPARATION
MINIMUM SEPARATION
SYMBOL
ECCENTRICITY
5 %
22 %
44 %
62 %
74 %
HEAT TRANSFER PARAMETER ($\frac{Nu}{Pr^{1/3}}$)
400
350
300
250
200
150
100
90
80
70
60
20,000
40,000
60,000
80,000
100,000
120,000
140,000
REYNOLDS NUMBER (Re)

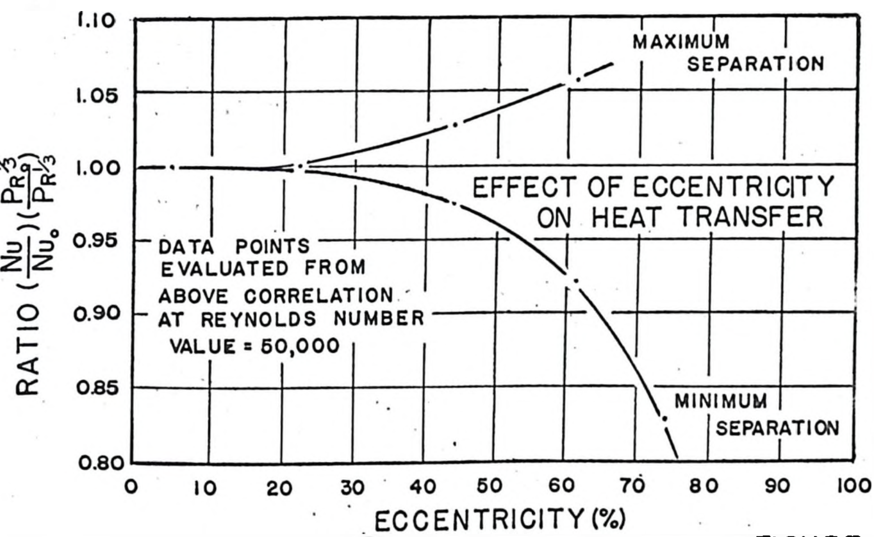
MAXIMUM SEPARATION
EFFECT OF ECCENTRICITY ON HEAT TRANSFER
DATA POINTS EVALUATED FROM ABOVE CORRELATION AT REYNOLDS NUMBER VALUE = 50,000
MINIMUM SEPARATION
RATIO ($\frac{Nu}{Nu_o}$)($\frac{Pr_o^{1/3}}{Pr^{1/3}}$)
1.10
1.05
1.00
0.95
0.90
0.85
0.80
0
10
20
30
40
50
60
70
80
90
100
ECCENTRICITY (%)

FIGURE #9

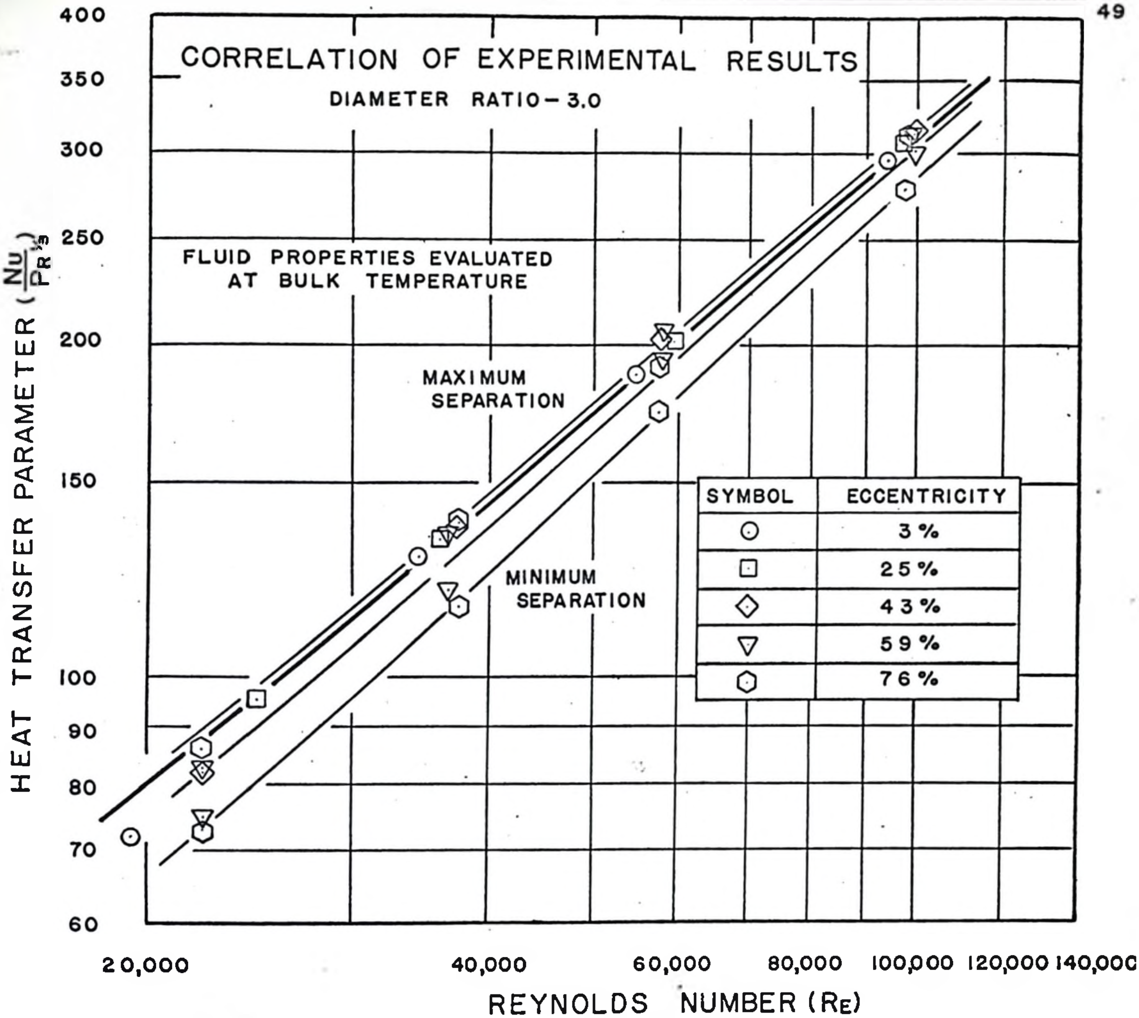
CORRELATION OF EXPERIMENTAL RESULTS
DIAMETER RATIO – 3.0
FLUID PROPERTIES EVALUATED AT BULK TEMPERATURE
MAXIMUM SEPARATION
MINIMUM SEPARATION
SYMBOL
ECCENTRICITY
3 %
25 %
43 %
59 %
76 %
HEAT TRANSFER PARAMETER ($\frac{Nu}{Pr^{1/3}}$)
400
350
300
250
200
150
100
90
80
70
60
20,000
40,000
60,000
80,000
100,000
120,000
140,000
REYNOLDS NUMBER (RE)

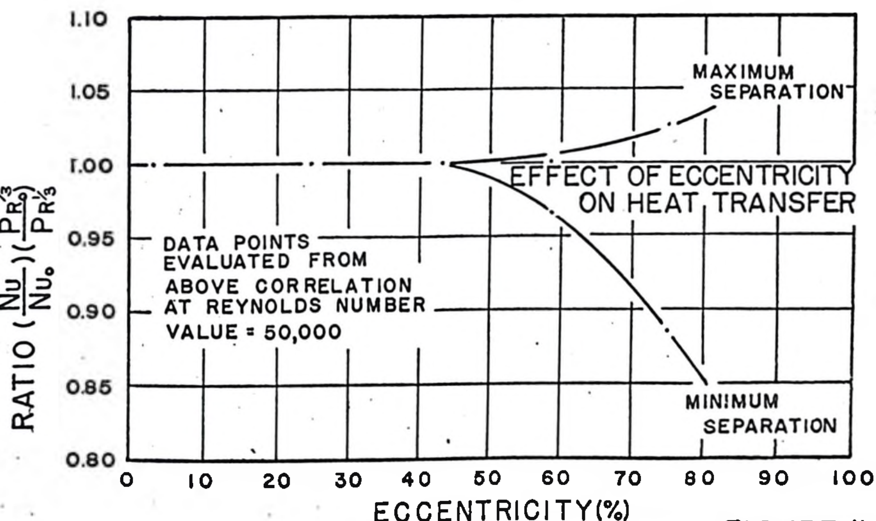
MAXIMUM SEPARATION
EFFECT OF ECCENTRICITY ON HEAT TRANSFER
DATA POINTS EVALUATED FROM ABOVE CORRELATION AT REYNOLDS NUMBER VALUE = 50,000
MINIMUM SEPARATION
RATIO ($\frac{Nu}{Nu_o}$)($\frac{Pr_o^{1/3}}{Pr^{1/3}}$)
1.10
1.05
1.00
0.95
0.90
0.85
0.80
0
10
20
30
40
50
60
70
80
90
100
ECCENTRICITY(%)

FIGURE # 10

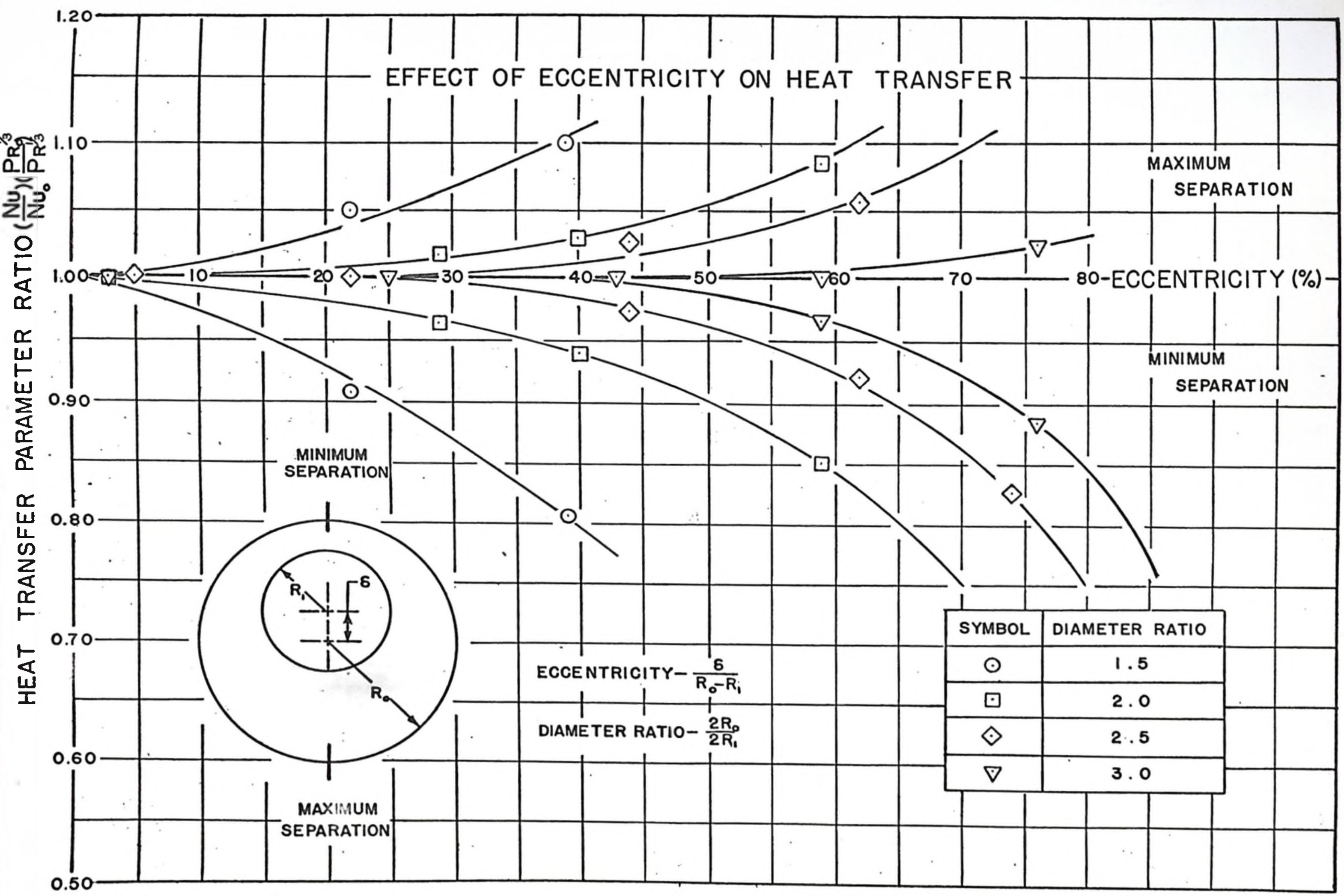
EFFECT OF ECCENTRICITY ON HEAT TRANSFER
HEAT TRANSFER PARAMETER RATIO $\left(\frac{Nu}{Nu_o}\right)\left(\frac{PR_o^{1/3}}{PR^{1/3}}\right)$
1.20
1.10
1.00
0.90
0.80
0.70
0.60
0.50
10
20
30
40
50
60
70
80
ECCENTRICITY (%)
MAXIMUM SEPARATION
MINIMUM SEPARATION
MINIMUM SEPARATION
MAXIMUM SEPARATION
R_i
δ
R_o
ECCENTRICITY – $\frac{\delta}{R_o - R_i}$
DIAMETER RATIO – $\frac{2R_o}{2R_i}$
SYMBOL
DIAMETER RATIO
1.5
2.0
2.5
3.0

FIGURE # 11

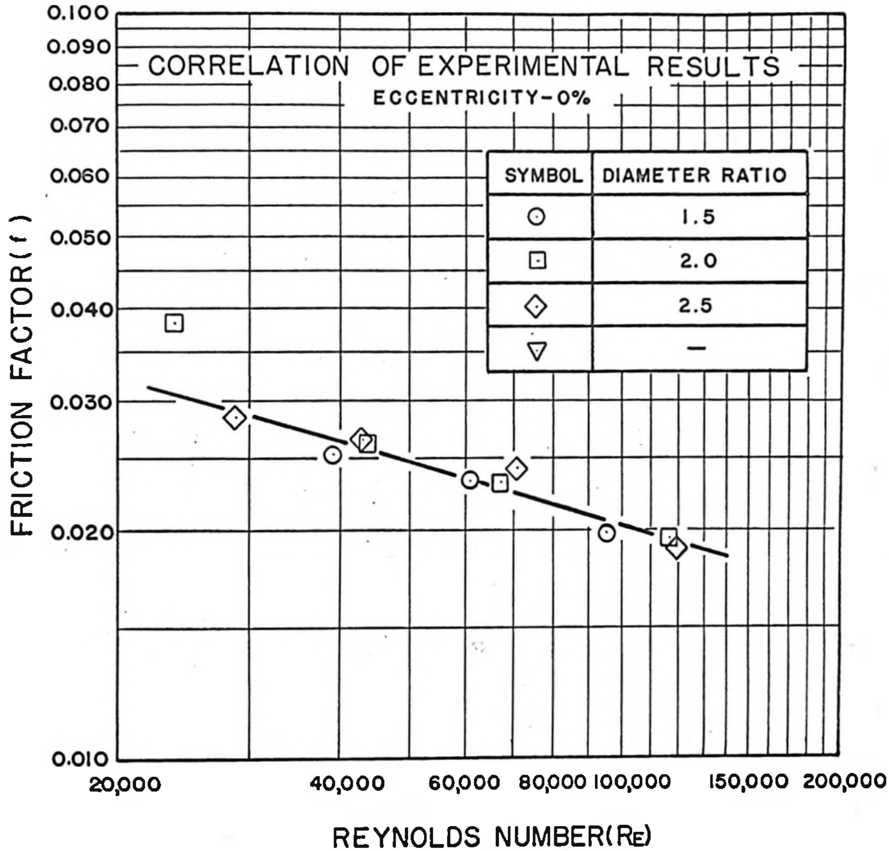
CORRELATION OF EXPERIMENTAL RESULTS
ECCENTRICITY-0%
SYMBOL
DIAMETER RATIO
1.5
2.0
2.5
—
FRICTION FACTOR(f)
0.100
0.090
0.080
0.070
0.060
0.050
0.040
0.030
0.020
0.010
20,000
40,000
60,000
80,000
100,000
150,000
200,000
REYNOLDS NUMBER(RE)

FIGURE # 12

APPENDIX

I TEST RESULTS

I.I MEASURED VALUES

DIAMETER RATIO	ECCENTRICITY (%)	FLOWRATE US GALLONS/MINUTE	POTENTIAL DROP OVER TEST SECTION VOLTS	CURRENT FLOWING THROUGH TEST SECTION AMPERES	PRESSURE DIFFERENCE OVER EFFECTIVE LENGTH "MERCURY	BULK TEMPERATURE OF WATER CIRCULATING THROUGH TEST SECTION: UPSTREAM °F	DOWNSTREAM °F	SURFACE TEMPERATURES MEASURED IN THE REGION OF FULLY DEVELOPED TURBULENT FORCED CONVECTION HEAT TRANSFER: MAXIMUM SEPARATION °F	°F	MINIMUM SEPARATION °F	°F
1.5	3	23.7	22.1	448	25.50	98.3	101.1	123.3	123.7	123.3	124.0
		14.8	19.2	387	11.55	99.4	102.6	124.3	125.0	125.0	125.7
		9.7	15.1	306	5.40	98.2	101.3	120.3	121.0	121.0	121.7
	22	23.7	21.7	441	24.80	103.2	106.0	127.0	126.7	127.3	127.3
		14.8	19.0	384	11.10	99.1	102.3	122.7	122.7	126.3	126.7
		9.4	16.4	327	5.00	100.0	104.0	125.3	125.3	129.7	129.7
	39	21.3	20.3	408	20.40	102.0	104.6	123.7	123.7	128.3	128.7
		14.8	17.8	359	10.95	99.9	102.6	122.0	122.3	126.7	126.7
		9.7	14.4	292	5.05	98.5	101.4	118.3	118.7	123.7	123.3
2.0	3	32.2	19.0	381	4.00	103.7	105.3	131.0	131.0	130.7	130.7
		18.6	16.1	324	1.59	100.8	102.6	129.7	129.7	130.0	130.0
		12.0	14.2	282	0.76	101.4	103.6	131.7	132.0	132.0	132.0
		6.7	10.8	215	0.34	101.9	104.2	131.0	131.3	131.0	131.3
	29	31.2	19.6	389	3.70	103.1	104.8	132.0	132.0	132.3	133.0
		18.3	17.1	341	1.56	102.4	104.4	134.0	134.0	135.3	135.3
		12.0	13.4	265	0.78	102.5	104.5	129.3	129.7	131.0	131.7
		6.5	10.7	214	0.32	101.0	103.1	129.7	130.0	132.3	132.3
	40	31.8	19.2	386	3.85	100.5	102.2	128.0	128.0	128.7	129.3
		18.4	16.4	332	1.56	99.6	101.6	130.7	130.7	131.7	131.7
		12.0	13.9	277	0.79	101.8	103.8	129.7	130.3	134.3	134.0
		6.7	11.0	215	0.33	100.0	102.2	129.7	129.7	136.0	135.7
	59	31.5	18.8	376	3.76	103.2	104.9	129.0	129.0	131.3	130.7
		18.5	16.6	333	1.58	102.1	104.0	131.3	131.3	134.3	134.0
		12.0	13.3	267	0.75	99.0	101.0	127.0	127.0	133.0	132.7
		6.7	10.7	214	0.35	99.4	101.6	128.0	128.0	137.3	136.7
2.5	5	38.0	17.3	344	1.17	103.7	104.8	132.3	132.3	131.3	132.3
		22.0	14.4	303	0.50	102.8	104.1	133.7	134.0	132.0	133.0
		13.9	12.4	244	0.22	101.6	103.0	133.3	134.0	132.3	132.7
		9.1	10.6	207	0.10	101.2	102.9	135.0	135.7	135.0	135.0
	22	37.0	16.9	336	1.23	102.4	103.5	130.7	130.7	130.0	130.3
		22.4	14.0	280	0.51	99.2	100.4	127.7	127.7	128.0	128.0
		13.9	12.7	254	0.29	99.0	100.4	132.3	132.0	133.0	133.0
		8.3	10.3	205	0.13	98.9	100.4	134.0	134.0	134.3	134.7
	44	36.6	17.6	347	1.09	103.3	104.4	132.7	133.0	132.0	133.3
		22.0	14.4	285	0.44	102.4	103.6	130.7	131.0	131.3	132.0
		13.5	11.5	228	0.21	102.0	103.3	128.3	129.3	130.3	130.7
		9.1	9.6	190	0.11	100.7	102.1	127.7	128.3	130.7	130.7
	62	37.6	17.7	352	1.12	103.4	104.5	132.3	132.7	133.3	133.3
		21.8	14.0	275	0.43	102.0	103.1	129.0	129.3	131.0	131.0
		13.9	11.6	228	0.23	100.7	102.0	127.7	127.7	130.7	130.0
		8.3	9.2	182	0.08	100.5	101.8	126.7	126.7	132.3	130.7
	74	37.0	17.3	344	1.32	103.5	104.7	132.7	133.0	134.7	134.0
		21.3	14.6	287	0.52	101.4	102.7	133.0	133.3	135.3	135.3
		13.9	11.9	233	0.27	102.4	103.7	130.3	130.7	137.0	137.0
		8.9	9.5	185	0.13	103.6	105.0	131.3	131.3	138.0	138.0
3.0	3	39.0	15.1	285	—	103.8	104.5	133.3	133.3	132.7	133.3
		22.4	12.6	237	—	104.5	105.5	135.7	136.0	135.3	135.7
		14.6	10.9	204	—	102.2	103.2	134.7	135.3	135.3	135.7
		8.3	8.3	156	—	101.2	102.2	136.0	135.0	135.0	134.7
	25	42.0	15.9	303	—	99.2	100.1	130.7	130.7	129.7	130.3
		24.7	14.0	264	—	103.2	104.2	138.7	139.7	139.0	139.0
		15.6	11.5	219	—	99.5	100.6	135.0	135.7	135.3	135.0
		10.8	9.6	180	—	99.9	101.0	133.0	134.0	134.3	134.0
	43	42.0	15.8	300	—	102.1	103.0	133.0	133.0	131.3	132.0
		24.4	13.1	249	—	102.1	103.0	133.7	133.7	133.3	133.0
		16.1	10.6	201	—	100.2	101.1	129.3	129.3	129.7	130.0
		9.4	8.4	159	—	102.8	103.8	132.7	132.7	134.7	133.7
	59	42.2	16.7	318	—	101.1	102.0	135.7	135.7	135.7	136.7
		25.0	13.8	264	—	100.0	101.0	135.3	136.0	136.7	137.7
		15.8	11.9	225	—	100.2	101.3	137.3	138.3	141.0	142.3
		9.7	9.5	180	—	99.0	100.2	136.7	138.3	141.7	141.7
	76	40.4	15.0	285	—	103.3	104.1	132.7	133.3	132.7	134.0
		24.4	12.0	228	—	101.5	102.3	129.0	129.7	131.0	132.0
		15.7	11.3	212	—	102.7	103.8	136.0	137.7	141.0	141.0
		9.4	8.4	159	—	102.4	103.4	131.0	132.7	136.0	137.0
3.5	2	55.0	15.3	305	—	99.4	100.1	131.0	131.3	131.0	131.3
		30.8	12.4	246	—	97.3	98.0	129.3	129.7	129.3	129.7
		19.8	9.9	199	—	97.1	97.8	127.3	127.3	127.3	127.7
		11.7	8.7	174	—	98.0	98.8	134.3	134.3	134.0	134.3
4.0	6	55.0	12.8	253	—	100.2	100.7	128.7	128.3	127.3	127.7
		32.0	10.6	211	—	103.7	104.2	132.7	132.7	131.3	131.7
		26.0	9.5	186	—	100.0	100.5	128.3	128.3	127.0	127.7
		12.5	7.7	150	—	99.8	100.3	133.7	133.0	133.0	133.3

1.2 DERIVED RESULTS

DIAMETER RATIO	ECCENTRICITY (%)	HEAT FLUX CALCULATED FROM ELECTRICAL MEASURE. BTU/HR-FT.^{2}	HEAT FLUX CALCULATED FROM CALORIMETRIC MEASURE. BTU/HR-FT.^{2}	TEMPERATURE DROP IN STAINLESS STEEL TUBE °F	MEAN FILM TEMPERATURE DIFFERENCE °F: MAXIMUM SEPARATION	MEAN FILM TEMPERATURE DIFFERENCE °F: MINIMUM SEPARATION	FORCED CONVECTION HEAT TRANSFER COEFFICIENT BTU/HR-FT^2-F: MAXIMUM SEPARATION	FORCED CONVECTION HEAT TRANSFER COEFFICIENT BTU/HR-FT^2-F: MINIMUM SEPARATION	MOODY FRICTION FACTOR —
1.5	3	127,500	127,000	5.4	18.1		7040		.0198
		95,700	97,200	4.1	19.6		4880		.0231
		59,500	61,100	2.5	18.4		3240		.0252
	22	123,400	125,500	5.2	16.2	17.2	7620	7160	.0193
		93,800	93,400	4.0	17.5	21.3	5370	4410	.0222
		69,000	76,200	2.9	20.0	24.3	3450	2840	.0248
	39	106,800	107,200	4.5	15.3	18.8	6980	5730	.0197
		82,200	79,200	3.5	17.0	20.5	4840	4000	.0219
		54,100	57,900	2.3	15.6	20.0	3470	2700	.0236
2.0	3	93,000	95,700	4.0	22.2		4200		.0195
		67,000	64,500	2.9	26.0		2580		.0232
		52,000	52,800	2.2	27.0		1910		.0264
		29,900	32,400	1.3	26.2		1140		.0384
	29	98,400	99,000	4.2	23.6	24.3	4170	4050	.0193
		75,000	72,100	3.2	27.0	28.4	2790	2640	.0236
		45,700	47,800	1.9	23.7	25.6	1930	1785	.0272
		29,500	31,200	1.3	25.9	28.7	1140	1030	.0384
	40	95,400	101,000	4.0	22.1	23.4	4320	4080	.0193
		72,200	72,100	3.1	25.8	27.6	2800	2620	.0234
		49,600	48,000	2.1	24.8	29.5	2000	1680	.0278
		30,500	31,000	1.3	26.9	33.3	1130	910	.0372
	59	90,900	101,000	3.9	21.7	23.8	4190	3820	.0192
		71,100	69,100	3.0	25.0	28.0	2840	2540	.0234
		45,700	48,100	2.0	25.0	30.5	1820	1495	.0264
		29,500	30,900	1.2	26.0	36.4	1135	810	.0395
2.5	5	76,500	76,500	3.2	24.5		3120		.0190
		56,400	55,100	2.6	27.0		2090		.0244
		38,900	38,600	1.7	28.7		1355		.0266
		28,300	31,800	1.2	31.8		890		.0283
	22	73,200	75,100	3.1	24.3		3010		.0210
		50,500	51,600	2.1	25.7		1970		.0238
		41,500	38,800	1.8	31.1		1330		.0352
		27,100	25,800	1.1	33.4		810		.0440
	44	78,400	74,400	3.3	25.3	25.8	3110	3040	.0190
		52,800	50,500	2.2	25.3	26.4	2080	2000	.0213
		33,800	34,900	1.4	24.2	26.4	1395	1280	.0270
		23,500	26,300	1.0	25.4	28.5	925	825	.0311
	62	80,200	76,100	3.4	24.9	26.4	3230	3040	.0190
		49,500	46,200	2.1	24.4	26.7	2030	1860	.0211
		34,100	35,800	1.4	24.8	28.0	1370	1215	.0266
		21,500	22,500	0.9	24.7	30.3	875	710	.0272
	74	76,800	82,500	3.3	25.2	27.7	3040	2770	.0225
		53,900	53,500	2.3	28.4	32.8	1900	1645	.0267
		35,700	35,900	1.5	26.0	32.9	1380	1090	.0314
		22,600	25,500	1.0	26.1	34.0	870	665	.0385
3.0	3	55,500	50,200	2.3	26.4		2100		—
		38,500	41,500	1.6	28.8		1335		—
		28,500	29,100	1.2	31.2		915		—
		16,650	17,100	0.7	32.6		510		—
	25	61,800	69,400	2.6	28.0		2210		—
		47,500	46,200	2.0	33.2		1430		—
		32,400	33,800	1.4	33.9		955		—
		22,300	24,100	0.9	32.5		685		—
	43	61,000	69,300	2.6	27.2		2250		—
		42,200	41,900	1.8	21.9		1445		—
		27,300	28,400	1.2	27.8		985		—
		17,100	19,000	0.7	29.4		580		—
	59	68,000	70,500	2.9	30.7	31.7	2230	2160	—
		47,000	47,900	2.0	31.8	33.6	1475	1400	—
		34,400	34,100	1.4	39.6	35.5	970	870	—
		22,000	23,600	0.9	36.9	40.9	595	535	—
	76	55,000	59,900	2.3	26.6	27.9	2070	1970	—
		35,200	37,300	1.5	25.8	28.5	1370	1240	—
		30,700	33,800	1.3	31.9	37.1	975	830	—
		17,100	19,200	0.7	27.9	32.9	615	520	—
3.5	2	60,100	67,500	2.5	28.9		2080		—
		39,200	40,400	1.7	30.0		1310		—
		25,400	27,000	1.1	28.8		880		—
		19,350	19,000	0.8	35.0		555		—
4.0	6	41,700	49,200	1.8	25.6		1630		—
		28,700	29,900	1.2	26.9		1065		—
		22,600	24,800	1.0	26.7		850		—
		14,800	12,600	0.6	32.7		450		—

1.3 DIMENSIONLESS PARAMETERS

DIAMETER RATIO	ECCENTRICITY (%)	FLUID PROPERTIES EVALUATED AT BULK TEMPERATURE				FLUID PROPERTIES EVALUATED AT FILM TEMPERATURE			
		REYNOLDS NUMBER	NUSSELT NUMBER MAXIMUM SEPARATION	NUSSELT NUMBER MINIMUM SEPARATION	PRANDTL NUMBER	REYNOLDS NUMBER	NUSSELT NUMBER MAXIMUM SEPARATION	NUSSELT NUMBER MINIMUM SEPARATION	PRANDTL NUMBER
1.5	3	87,400	405		454	96,200	401		408
		55,300	281		447	61,100	278		398
		35,900	186		454	39,400	185		408
	22	92,000	437	411	429				
		55,200	310	255	448				
		35,600	199	164	440				
	39	79,200	402	327	435				
		55,400	279	231	447				
		35,900	200	154	454				
2.0	3	104,200	482		430	118,000	475		373
		57,600	298		450	67,300	293		377
		38,000	222		440	43,700	217		373
		21,500	131		434	24,000	129		383
	29	100,000	479	465	433				
		58,600	320	303	435				
		38,400	222	206	433				
		20,500	131	118	442				
	40	99,200	497	469	446				
		57,400	322	302	447				
		38,100	229	193	438				
		20,700	130	105	447				
	59	101,100	480	438	431				
		58,300	326	291	442				
		36,800	210	172	453				
		20,000	131	94	450				
2.5	5	104,800	538		431	120,000	528		371
		60,200	359		435	71,100	355		370
		37,500	234		441	43,500	230		373
		24,500	154		442	28,800	150		368
	22	100,700	5,18		438				
		58,900	341		456				
		36,500	230		456				
		21,800	140		457				
	44	100,300	536	522	434				
		59,800	360	345	438				
		36,600	242	221	440				
		24,300	160	142	447				
	62	103,700	556	523	433				
		59,200	362	322	440				
		37,100	238	211	447				
		22,200	151	123	447				
	74	101,900	522	476	433				
		57,300	328	284	4.42				
		38,000	238	188	438				
		24,600	149	115	430				
30	3	93,900	484		433	107,900	474		370
		54,500	305		428	63,000	301		362
		34,500	210		440	40,600	206		368
		19,500	117		445	22,900	116		370
	25	96,700	509		457				
		59,100	328		435				
		36,000	221		454				
		24,800	158		453				
	43	99,600	516		442				
		57,700	333		442				
		37,400	227		452				
		22,300	134		436				
	59	99,400	513	497	447				
		58,000	340	322	452				
		36,600	222	199	450				
		22,300	138	124	457				
	76	97,400	477	453	434				
		57,300	316	285	443				
		37,500	224-	190	437				
		22,300	141	119	437				
35	2	112,200	600		457	131,300	588		380
		61,300	378		470	72,400	371		388
		39,200	255		471	46,100	250		393
		23,600	160		465	28,700	156		377
40	6	104,000	563		452	117,400	555		382
		61,500	367		433	70,500	362		372
		48,000	293		455	55,300	289		386
		23,000	156		455	27,200	154		376

2. THEORETICAL DERIVATIONS

2.1 TEMPERATURE DROP IN THE WALL OF A STAINLESS STEEL TUBE

THE DIFFERENTIAL EQUATION

$$\frac{d^2T}{dr^2} + \frac{1}{r}\frac{dT}{dr} + \frac{Q'''}{k_{S.S.}} = 0 \qquad \text{—(1)}$$

IS POISSON'S EQUATION IN CYLINDRICAL CO-ORDINATES FOR STEADY STATE HEAT CONDUCTION IN A SOLID WITH HOMOGENEOUS INTERNAL HEAT GENERATION. EQUATION (1) CAN BE SOLVED BY SUBSTITUTING $\frac{dT}{dr} = T'$ AND $\frac{d^2T}{dr^2} = \frac{dT'}{dr}$.

$$\frac{dT'}{dr} + \frac{T'}{r} + \frac{Q'''}{k_{S.S.}} = 0 \qquad \text{—(2)}$$

EQUATION (2) HAS A CLASSICAL SOLUTION

$$T' = \mathrm{EXP}\left(-\int\frac{dr}{r}\right)\left[\int -\frac{Q'''}{k_{S.S.}}\mathrm{EXP}\left(+\int\frac{dr}{r}\right)dr + \lambda\right]$$

$$= \mathrm{EXP}(-\ln r)\left[\int -\frac{Q'''}{k_{S.S.}}\mathrm{EXP}(+\ln r)dr + \lambda\right]$$

$$= \frac{1}{r}\left[\int -\frac{Q'''}{k_{S.S.}}r\,dr + \lambda\right] = -\frac{Q'''}{k_{S.S.}} \times \frac{r}{2} + \frac{\lambda}{r} \qquad \text{—(3)}$$

FOR A HOLLOW CYLINDER WITH AN ADIABATIC INNER SURFACE, $T' = 0$ WHEN $r = r_i$. APPLYING THIS CONDITION, GIVES

$$0 = -\frac{Q'''}{k_{S.S.}} \times \frac{r_i}{2} + \frac{\lambda}{r_i} \quad \text{AND} \quad \lambda = +\frac{Q'''}{k_{S.S.}} \times \frac{r_i^2}{2} \qquad \text{—(4)}$$

CONSEQUENTLY,

$$T' = -\frac{Q'''}{2k_{S.S.}}\left[r - \frac{r_i^2}{r}\right] \qquad \text{—(5)}$$

INTEGRATING EQUATION (5) AND APPLYING THE CONDITIONS THAT $T = T_o$ WHEN $r = r_o$ AND THAT $T = T_i$ WHEN $r = r_i$, GIVES

$$[T]_{T_i}^{T_o} = -\frac{Q'''}{2k_{S.S.}}\left[\frac{r^2}{2} - r_i^2 \ln r\right]_{r_i}^{r_o}$$

$$T_i - T_o = +\frac{Q'''}{2k_{S.S.}}(r_o^2 - r_i^2)\left[\frac{1}{2} - \frac{r_i^2}{r_o^2 - r_i^2}\ln\frac{r_o}{r_i}\right] \qquad \text{—(6)}$$

BUT $Q''' = \frac{Q}{A} \times \frac{\text{SURFACE AREA}}{\text{VOLUME}} = \frac{Q}{A} \times \frac{2\pi r_o L}{\pi(r_o^2 - r_i^2)L}$

$$= 2\frac{r_o}{(r_o^2 - r_i^2)} \times \frac{Q}{A} \qquad \text{—(7)}$$

THEREFORE, SUBSTITUTING EQUATION (7) INTO EQUATION (6)

$$T_i - T_o = +\frac{r_o}{k_{S.S.}}\left[\frac{1}{2} - \frac{r_i^2}{(r_o^2 - r_i^2)}\ln\frac{r_o}{r_i}\right] \times \frac{Q}{A} \qquad \text{— (8)}$$

2.2 SUPPORT LEG LENGTHS

DIAMETER RATIO $\frac{D_o}{D_i} = \frac{2R_o}{2R_i}$

ECCENTRICITY $\epsilon = \frac{\delta}{R_o - R_i}$

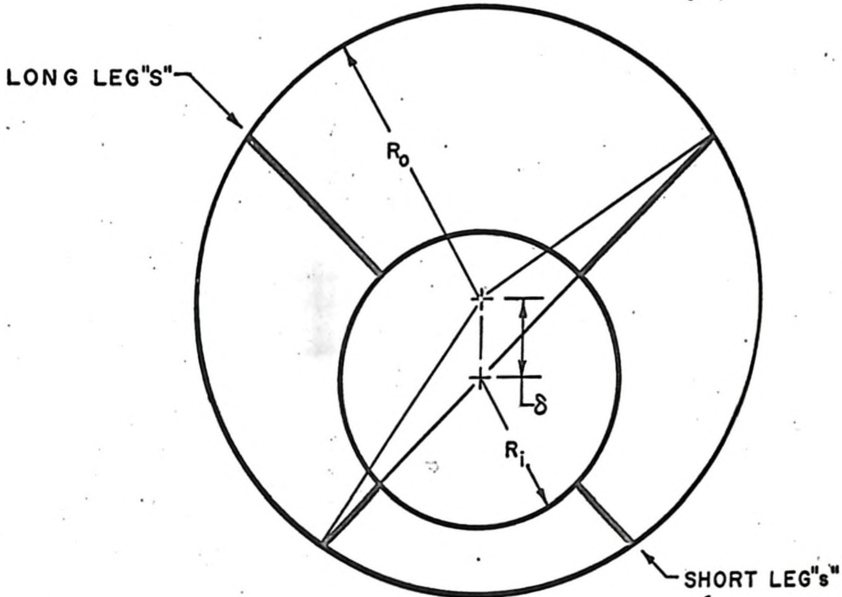

$$\sin\alpha = \frac{\delta \sin 45°}{R_o}$$

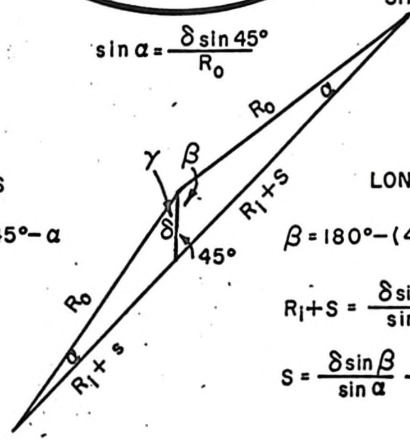

SHORT LEGS

$$\gamma = 180° - (135° + \alpha) = 45° - \alpha$$

$$R_i + s = \frac{\delta \sin\gamma}{\sin\alpha}$$

$$s = \frac{\delta \sin\gamma}{\sin\alpha} - R_i$$

LONG LEGS

$$\beta = 180° - (45° + \alpha) = 135° - \alpha$$

$$R_i + S = \frac{\delta \sin\beta}{\sin\alpha}$$

$$S = \frac{\delta \sin\beta}{\sin\alpha} - R_i$$

$$S + s + 2R_i \gtrless 2R_o$$

3. HEAT TRANSFER IN AN ECCENTRICALLY ARRANGED SINGLE-PASS SHELL-AND-TUBE HEAT EXCHANGER

Statement

A single-pass countor flow shell and tube heat exchanger with 4 square feet of heat transfer surface area is comprised of an inner tube 0.50" O.D. x 0.020" W.T. eccentrically located within an outer tube 1.25" O.D. x 0.125" W.T. The arrangement of the tubes is such that the eccentricity of the assembly is 60%. Oil at 155°F which flows through the inner tube at the rate of 32,000 lb/hr exchanges heat with water at 90°F which flows through the annular passage between the inner tube and outer tube at the rate of 8,000 lb/hr. Neglecting the thermal resistance of the wall of the inner tube, calculate

(a) The rate at which heat is exchanged.

(b) The approximate circumferential temperature variation in the wall of the inner tube at a plane midway between the ends of the heat exchanger.

Solution

(a) The solution of this problem is obtained through the use of plots of heat exchanger effectiveness η as a function of the hourly heat capacity ratio $\frac{(WC)\ min}{(WC)\ max}$ and the number of transfer units $\frac{AU}{(WC)\ min}$. Such a plot for a single-pass counter flow heat exchanger is presented below.

HEAT EXCHANGER OPERATING CHARACTERISTICS

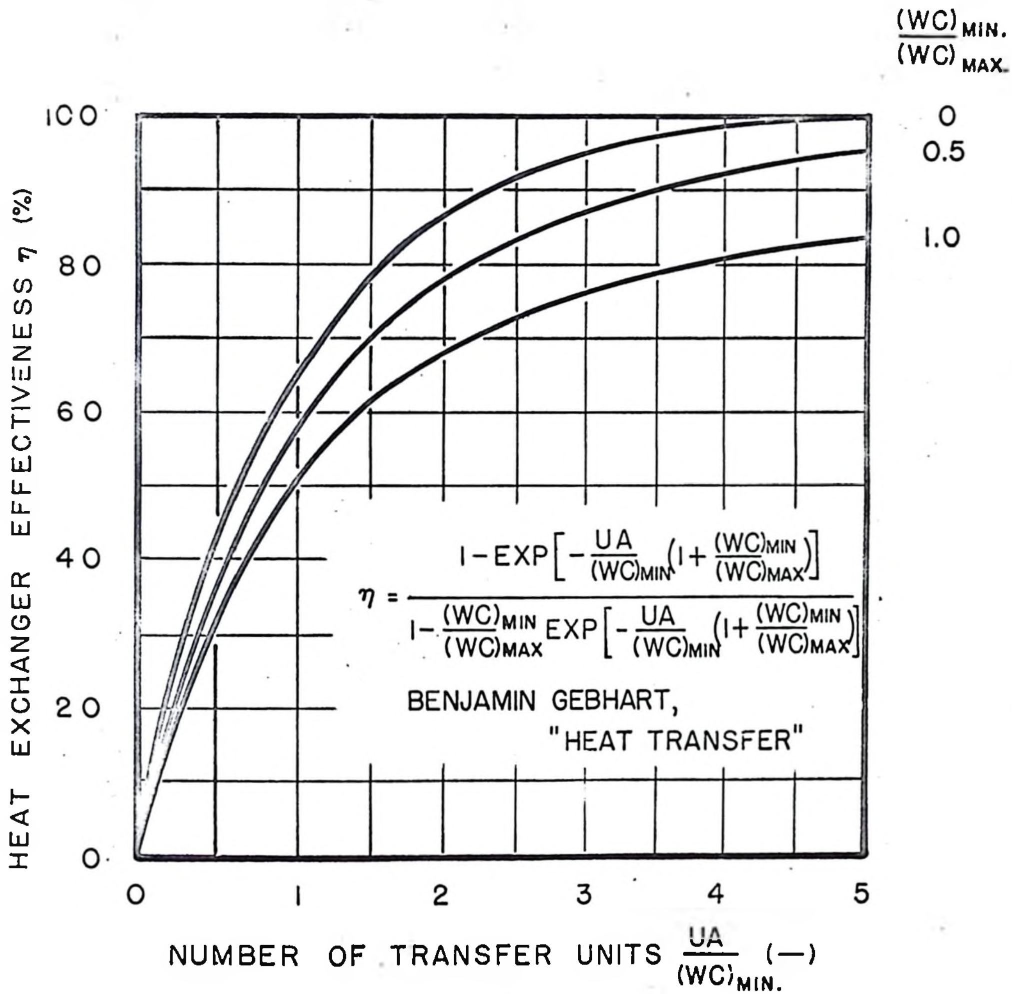

By definition, the rate at which heat is exchanged

$$Q = \eta\,(WC)_{min}\left[(T_{oil})_i - (T_{water})_i\right]$$

Oil

$(WC) = 32{,}000 \times 0.5 = 16{,}000\ \frac{B.T.U.}{hr^{o}F}$

The heat transfer coefficient at the inner surface of the tube separating the oil and water is computed by

$Nu = 0.023\,(Re)^{0.8}\,(Pr)^{0.4}$

using fluid properties evaluated at $150^{o}F$. Thus

$Re = \frac{4}{\pi} \times \frac{32{,}000}{54.3 \times 3600} \times \frac{12}{0.460} \times \frac{10^5}{9.8}$

$= 55{,}400$

$Pr = 122$

$h_i = 0.023 \times \frac{0.075 \times 12}{0.460} \times$

$(55{,}400)^{0.8}\,(122)^{0.4}$

$= 1920\,\frac{B.T.U.}{hr.ft^{2o}F}$

Note: It was assumed that $\mathcal{J}(50{,}000, 2.0, 60\%)$ was the numerical average of ζ evaluated at the locations of maximum and minimum separation.

Hence $\mathcal{J}(50{,}000, 2.0, 60\%) =$

$\frac{172 + 138}{2} = 155$

Water

$(WC) = 8{,}000 \times 1.0 = 8{,}000\ \frac{B.T.U.}{hr^{o}F}$

The heat transfer coefficient at the outer surface of the tube separating the oil and water is computed by

$Nu = \mathcal{J}\left(Re, \frac{D_o}{D_i}, \varepsilon\right) Pr^{1/3}$

using fluid properties evaluated at $100^{o}F$. Thus

$Re = \frac{4}{\pi} \times \frac{8{,}000}{60.6 \times 3600} \times \frac{12}{1.50} \times \frac{10^5}{0.74}$

$= 50{,}000$

$Pr = 4.52$

$h_o = \frac{0.364 \times 12}{0.500} \times$

$\mathcal{J}(50{,}000, 2.0, 60\%)\,(4.52)^{1/3}$

From Figure 8

Maximum Separation	Minimum Separation
$\zeta = \frac{Nu}{Pr^{1/3}} = 172$	$\zeta = \frac{Nu}{Pr^{1/3}} = 138$

$h_o = 8.70\left(\frac{172+138}{2}\right)(4.52)^{1/3}$

$= 2230\,\frac{B.T.U.}{hr.ft^{2o}F}$

$$\frac{(WC)min}{(WC)max} = \frac{8,000}{16,000} = 0.5$$

$$\frac{UA}{(WC)min} = \frac{4}{8,000}\left[\frac{1}{\frac{r_o}{r_i h_i} + \frac{1}{h_o}}\right] = \frac{1}{2000}\left[\frac{1}{\frac{0.25}{0.23 \times 1920} + \frac{1}{2230}}\right]$$

$$= \frac{1}{2,000}\left[\frac{1,000}{0.565 + 0.446}\right] = 0.5$$

η = 36.2% and $Q = 0.362 \times 8,000 \left[(155) - (90)\right] = 188,000 \frac{B.T.U.}{hr}$

The solution of the simultaneous linear differential equations governing the performance of the heat exchanger yields the temperature distributions shown below. The actual temperatures in the plane midway between the ends of the heat exchanger indicate that the temperatures chosen to evaluate the fluid properties were reasonable.

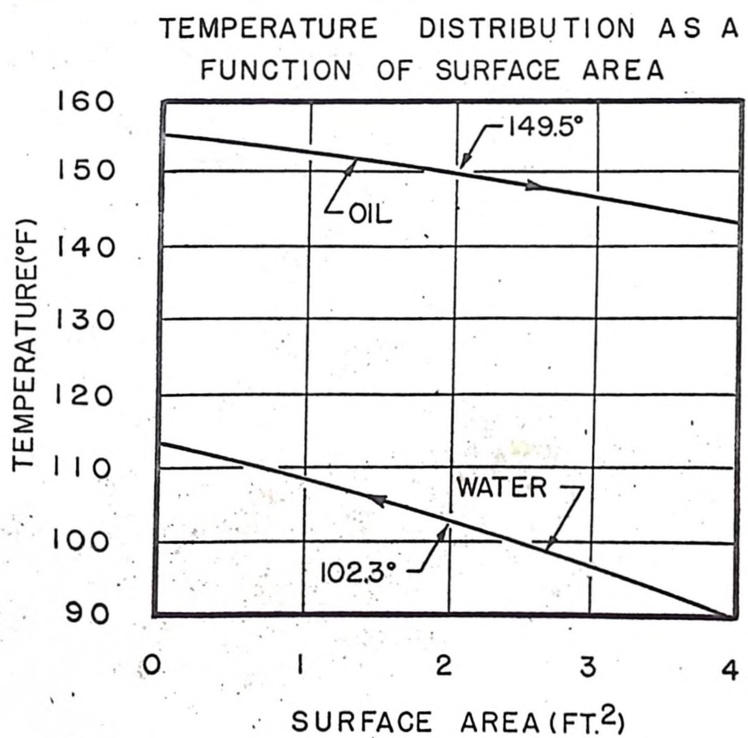

(b) The average temperature in the wall of the inner tube

$$T_{av} = 102.3 + \left[\frac{0.446}{0.565 + 0.446}\right] (149.5 - 102.3) = 123.1^{\circ}F$$

The maximum temperature in the wall of the inner tube occurring at the location corresponding to the minimum separation of the boundaries of the annular passage

$$T_{max} = 102.3 + \left[\frac{0.446 \times \frac{155}{138}}{0.565 + 0.446 \times \frac{155}{138}}\right] (149.5 - 102.3) = 124.5^{\circ}F$$

The minimum temperature in the wall of the inner tube occurring at the location corresponding to the maximum separation of the boundaries of the annular passage

$$T_{min} = 102.3 + \left[\frac{0.446 \times \frac{155}{172}}{0.565 + 0.446 \times \frac{155}{172}}\right] (149.5 - 102.3) = 121.9^{\circ}F$$

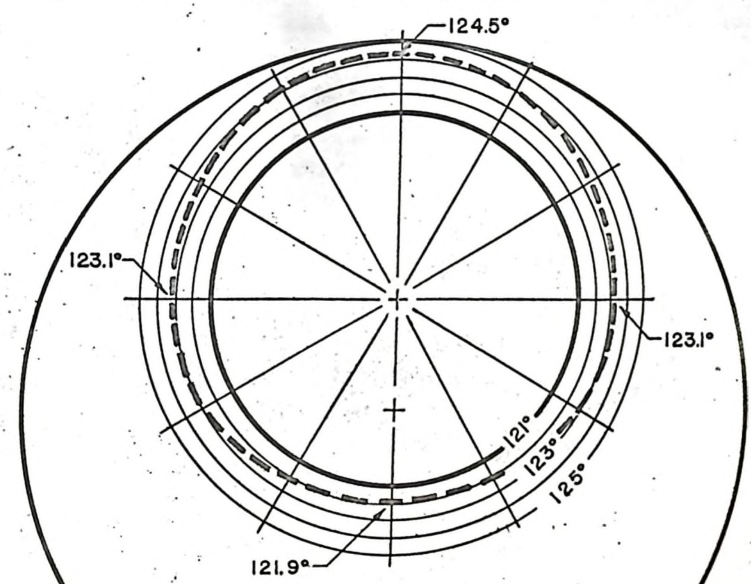

TEMPERATURE DISTRIBUTION
IN A PLANE MIDWAY BETWEEN
THE ENDS OF THE HEAT EXCHANGER